Biochemistry

Editors' Choice
Open Access

pubs.acs.org/biochemistry

Review

Metals in Motion: Understanding Labile Metal Pools in Bacteria

Published as part of Biochemistry special issue "A Tribute to Christopher T. Walsh".

John D. Helmann*

Cite This: *Biochemistry* 2025, 64, 329–345

Read Online

ACCESS | Metrics & More | Article Recommendations

ABSTRACT: Metal ions are essential for all life. In microbial cells, potassium (K^+) is the most abundant cation and plays a key role in maintaining osmotic balance. Magnesium (Mg^{2+}) is the dominant divalent cation and is required for nucleic acid structure and as an enzyme cofactor. Microbes typically require the transition metals manganese (Mn), iron (Fe), copper (Cu), and zinc (Zn), although the precise set of metal ions needed to sustain life is variable. Intracellular metal pools can be conceptualized as a chemically complex mixture of rapidly exchanging (labile) ions, complemented by those reservoirs that exchange slowly relative to cell metabolism (sequestered). Labile metal pools are buffered by transient interactions with anionic metabolites and macromolecules, with the ribosome playing a major role. Sequestered metal pools include many metalloproteins, cofactors, and storage depots, with some pools redeployed upon metal depletion. Here, I review the size, composition, and dynamics of intracellular metal pools and highlight the major gaps in understanding.

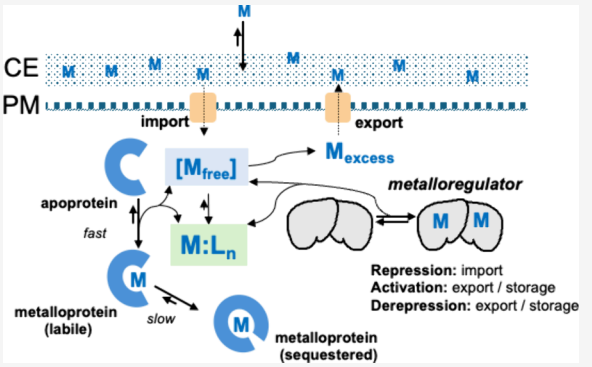

KEYWORDS: *metal physiology, metallomics, metalloregulation, metallochaperone, ribosome, labile metal pool*

INTRODUCTION

Microbial physiology relies on the ability of cells to obtain and exploit the ions needed to support macromolecular structure, enzyme catalysis, charge neutralization, and osmotic balance, all while avoiding toxicity.[1,2] Metal homeostasis relies on the regulation of import and export processes that help sustain a pool of kinetically labile metal complexes that can be accessed by nascent metalloproteins and to support metal-dependent processes.[3] However, the precise nature of the labile metal pool is still not fully understood and retains an aura of mystery. Here, I seek to define the major intracellular metal ion pools with an emphasis on what is and is not known regarding the molecular interactions that contribute to metal buffering, trafficking, and sequestration.

Much of our knowledge of labile metal pools comes from studies of model systems, including *Escherichia coli* and *Bacillus subtilis*,[1,4] but I will strive to highlight those features that are broadly conserved. We will focus on representatives of the three major classes of metal ions. The bulk ions (K^+, Mg^{2+}) have a low affinity for ligands and a large labile pool,[5,6] with most bacteria having total concentrations (quotas) of >100 mM.[7−9] The transition metals Mn^{2+} and Fe^{2+} (the dominant oxidation state in the labile pool) have a moderate affinity for ligands and cells have lower quotas (often ∼0.1 to 1 mM).[1,10,11] These ions are partitioned between complexes with a wide range of affinities and exchange kinetics, including a small subset (∼1%) present as free ions. Zn^{2+} and Cu^+ have a high affinity for ligands, with small labile pools and no free, fully hydrated ions at equilibrium.[3,12] The chemistry of the biologically relevant transition metal ions is dominated by their coordination in molecular complexes, which can be relatively inert (sequestered) or labile.[2] The latter pools include diverse complexes that are in equilibrium through ligand exchange reactions (Figure 1). These universal chemical properties dictate metal physiology throughout biology.

Historical Context: Bioinorganic Foundations of Microbial Metal Ion Physiology. The properties of metal ions have long fascinated chemists. One early insight, familiar to chemistry students, is the notion that crystals of table salt (NaCl) dissolve in water to form spatially separated, hydrated ions with the Na^+ stabilized by ion-dipole interactions with H_2O. While the imprint of this idea remains strong, and in retrospect it seems intuitive, the original presentation was met with fierce resistance. In the late 19th century, Svante Arrhenius presented his theory of ion dissociation as the basis for the electrical conduction properties of salt solutions to a highly skeptical

Received: October 28, 2024
Revised: December 2, 2024
Accepted: December 13, 2024
Published: January 5, 2025

https://doi.org/10.1021/acs.biochem.4c00726
Biochemistry 2025, 64, 329−345

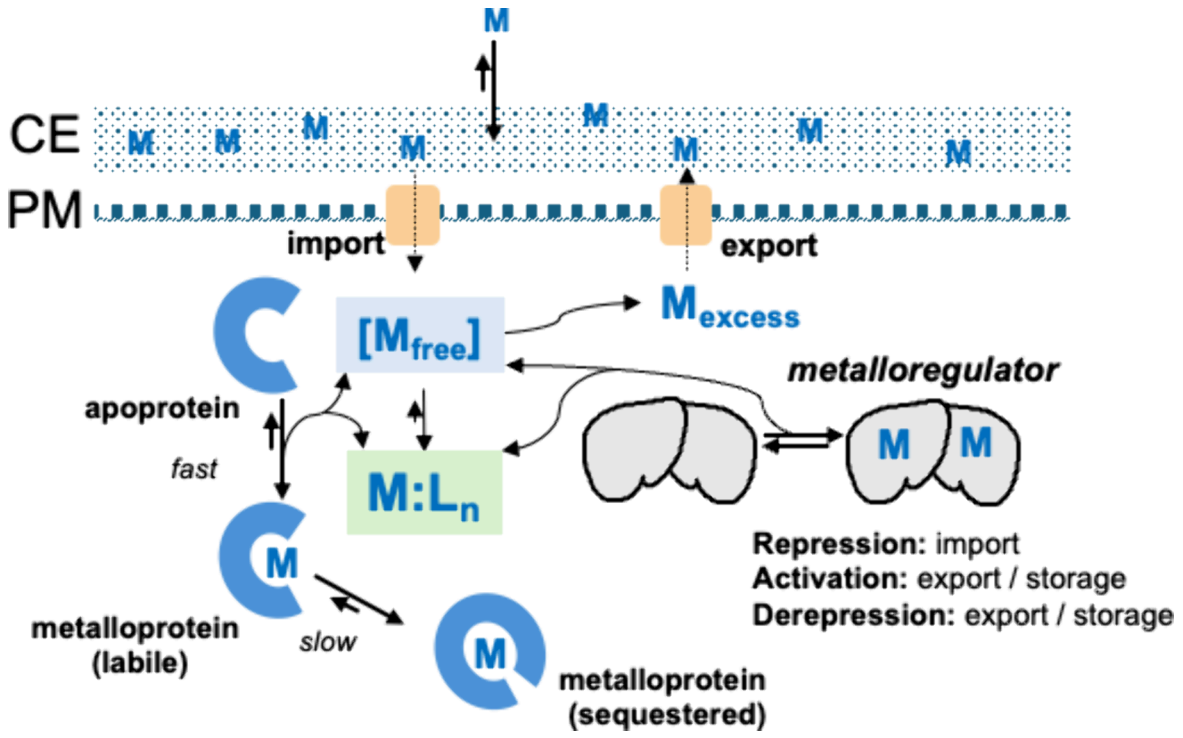

Figure 1. Overview of metal mobility in bacterial cells. Metal ions (M) from the environment are often concentrated by ionic interactions with the anionic components of the cell envelope (CE), including the outer membrane (in Gram-negative bacteria) and the peptidoglycan cell wall and associating anionic polymers. Transporters in the plasma membrane (PM) mediate the energy-dependent import and export of metals. Imported ions populate an equilibrating labile pool, which includes free, aquated metal ions (M_{free}; blue), metal–ligand complexes ($M:L_n$; green), and labile metalloprotein complexes. Metalloproteins may bind metal ions tightly, or may form higher order complexes, that sequester ions away from water and other competing ligands. Metalloregulatory proteins sense the transitions between metal deficiency, sufficiency, and excess to alter gene expression. The sensitivity of metalloregulators for their cognate metal ligands provides an estimation of the M_{free} pool.

thesis committee (1884), and the referees only begrudgingly granted the PhD degree.[13] His insights were later recognized with the 1903 Nobel Prize in Chemistry. While Arrhenius' model was supported by many (the "ionists"), others (the "hydrationists") raised counterarguments and the field remained unsettled for many years.[14] Indeed, the ensuing debate illustrates how scientific models evolve over time, and provides ample fodder for teaching some of the central concepts of physical chemistry.[15]

In contrast with NaCl, other inorganic salts are sparingly soluble in water. Chemistry students may be familiar with the use solubility products (K_{sp}) to determine the levels of ions in solution at equilibrium. Such calculations, however, are not easily adapted to the complex conditions of the cytoplasm due to variable water activity and numerous competing ligands. Despite this limitation, considerations of ion solubility have been influential in understanding how life has adapted to changing metal availability over Earth's history. The oceans of early Earth were exposed to a reducing atmosphere and contained high levels of sulfide, which led to precipitation of insoluble copper sulfides (e.g., Cu_2S, $K_{sp} = 6.1 \times 10^{-49}$) whereas Fe^{2+} (ferrous iron) was readily available.[16,17] Following the great oxidation event, the availability of several transition metals changed significantly, with greater availability of copper and zinc, and substantially reduced levels of iron, which is largely oxidized to Fe^{3+} in aerobic environments. The poor solubility of Fe^{3+} at near neutral pH leads to equilibrium levels of free iron of $\sim 10^{-18}$ M, which is orders of magnitude below that needed by most microbes. The resultant iron limitation was a major driving force behind the evolution of high affinity siderophores to support iron nutrition.[18,19]

The metal ions relevant to biology have properties that span the range from highly available, with substantial pools of free ions (K^+ and Mg^{2+}), to those that have an average of less than one free ion per bacterial cell (Zn^{2+} and Cu^+).[3,20] Manganese and iron have intermediate properties. The tendency for metal ions in aqueous solution to interact tightly with ligands is summarized in the Irving-Williams series[21,22] (here augmented with Mg^{2+} and Cu^+): $Mg^{2+} < Mn^{2+} < Fe^{2+} < Co^{2+} < Ni^{2+} < Cu^{2+}$ (and Cu^+) > Zn^{2+}. Within the intracellular environment, metal ions are present in a myriad of coordination environments that range from tightly bound (sequestered) to highly mobile (labile) (Figure 1). Sequestered pools are relatively static and can be defined by their size and the composition and metal-binding affinities of their components. In contrast, the labile pool is a turbulent jumble of metal ions characterized by fleeting interactions with an ever-changing cast of ligands. An initial picture has emerged of how metals are distributed at equilibrium during balanced growth, but capturing the magnitude and kinetics of metal redistribution in response to sudden metal depletion or excess has proven challenging.

Metal Quotas and Pools. Considering this complexity, an agreed vocabulary is important. Here, I use **metal quota** to refer to the total cellular content of a metal ion, a term that originated with metal nutrition studies in marine systems.[23] The quota (expressed as atoms per cell or in molarity) typically includes both intracellular and envelope-associated ions and may include multiple oxidation states. I specify the ionic state in contexts where it is well-defined and use the name of the element when

https://doi.org/10.1021/acs.biochem.4c00726
Biochemistry 2025, 64, 329−345

referring to pools of mixed valence. The **labile metal** pool comprises that fraction of the intracellular quota that exchanges ligands on a fast time scale relative to cell metabolism and growth and therefore is considered **bioavailable**. This contrasts with the **sequestered metal** pool, which comprises metal ions that are tightly bound to their ligands and not exchanging on a rapid time scale. The boundary between labile and sequestered metal pools is arbitrary, and sequestration can be conditional. For example, sequestered metals may become bioavailable due to metal ion competition, changes in redox state, export from vacuoles, or mobilization from storage reservoirs.

The **free metal** pool refers to those ions that are fully hydrated at equilibrium (Figure 1). In relatively dilute systems, free metal concentrations can be estimated by calculations of chemical speciation. Within the more complex milieu of the cytosol, the biochemically determined metal sensitivity of metalloregulatory proteins and metal-sensing riboswitches provides a useful proxy[3,4] and defines the biological set-point for specific genetic changes (Figure 2).[4,24] For regulators of metal import, the set-point defines the boundary between metal deficiency and sufficiency, whereas for regulators of efflux and storage, the set-point delineates the boundary between sufficiency and excess.[1] In practice, the set-point often spans a range of values. For some regulatory proteins there are multiple metal-binding sites in the functional oligomer and these may bind with negative cooperativity.[25] Further, since metal binding to metalloregulators often affects DNA affinity, the converse is also true,[26] and these effects need to be considered when assessing sensitivity.[3,4] For example, Zur proteins sense Zn^{2+} sufficiency and the binding of Zn^{2+} is anywhere from 10- to 10^3-fold tighter when measured in the presence of DNA.[25,27,28]

The biologically important transition metals can all form metal-aquo coordination complexes, often with six, octahedrally arranged water molecules that exchange with bulk solvent on a microsecond time scale.[2] In the cytosol, some of this water may be displaced by oxygen, nitrogen, or sulfur atoms found in macromolecules and metabolites. The resulting complexes are often polydentate and include the many metalloproteins in the cell as well as common cofactors (e.g., heme, chlorophyll, cobamides, molybdenum cofactor). There is no shortage of metal ligands in the cell; ribosomes, RNA, DNA, proteins, nucleotides, amino acids, phospholipids, phosphosugars, and thiol-containing metabolites all play important roles. At equilibrium, free metal pools are significant for K^+ and Mg^{2+} and are composed of both free and weakly complexed ions.[5−7] Most manganese and iron is bound, but a small free pool is present and contributes to metal acquisition by nascent metalloproteins.[3] For Zn^{2+} and Cu^+, however, the notional free metal pool is less than one atom per cell at equilibrium, and the mobility of metals relies on ligand exchange chemistry.[3,31,32]

Metal Ions and the Intracellular Milieu. The biochemical processes that support life largely play out in the crowded milieu of the cell interior (Figure 3).[33] As a first approximation, the interior of the cell can be viewed as an aqueous solution nearly saturated with large and complex biological polymers (proteins, nucleic acids), metabolites, and ions. The physicochemical properties of the cell interior are vastly different from those of dilute aqueous solutions and are dominated by the high concentration of macromolecules that collectively occupy ∼30% of the cell volume.[34−36] Studies in *E. coli* reveal dominant contributions from proteins (200−320 mg/mL) and RNA (75−120 mg/mL) with DNA present at lower levels (11−18 mg/mL).[37] The remainder of the volume (∼50−70%) is water and

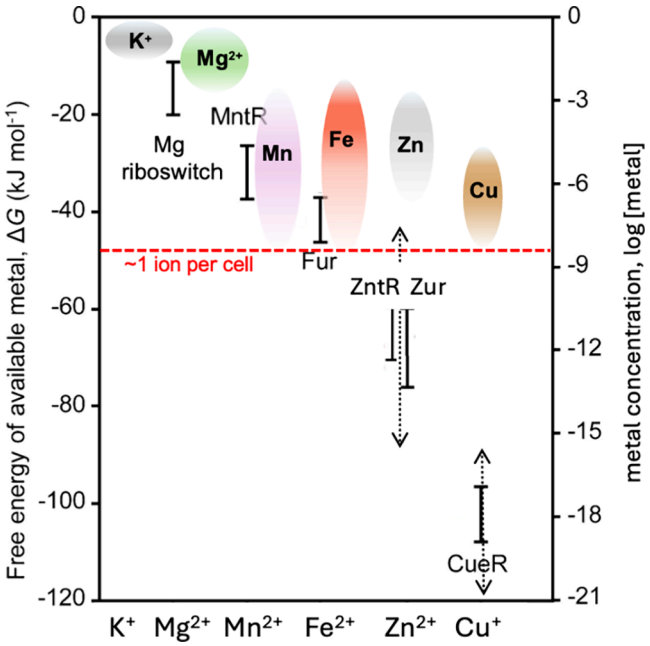

Figure 2. Metal ion quotas and buffered free metal concentrations. Colored ovals represent typical bacterial metal quotas (shown as metal concentrations; right axis): K^+ (gray) has a quota often in the range of 0.1 to near 1 M depending on environmental osmolarity, and Mg^{2+} (green) in the 100 mM range. The moderate affinity ions, manganese (purple) and iron (red), have variable quotas of up to 1 mM, with iron > manganese in most bacteria.[11] For the high affinity metals Zn^{2+} (light gray) levels are often 10 μM to 1 mM, whereas copper (brown) quotas are variable, but often lower than Zn^{2+}. Metal homeostasis relies on metalloregulators and riboswitches that sense the labile pool by reversible metal binding. Their sensitivity corresponds to a nominal concentration of free (aquated) ions (right axis) as calculated from the free energy change (ΔG, left axis) for the metal binding affinity needed to effect changes in gene expression.[3] The red dotted line is the concentration corresponding to one atom for a typical cell the size of *E. coli* or *B. subtilis*. The brackets denote the range of free metal concentrations corresponding to a 10−90% change in gene expression as calculated for the indicated metalloregulators purified from *Salmonella*[4] and the MgtE riboswitch from *B. subtilis*.[29] These values are comparable to those for other species. Sensitivity is determined by the affinity of the metalloregulator for its cognate ion and the effects of DNA-binding on metal affinity (thermodynamic coupling), as discussed in detail elsewhere.[26,30] Metalloregulation can be effective over a broad range (illustrated by the dashed lines for Zn^{2+} and Cu^+) due to differences in operator affinity and cooperative effects on both metal and DNA-binding. The figure is adapted with modifications from Foster et al.[3] (CC-BY-4.0 license), which can be consulted for further details.

dissolved solutes, including metabolites and inorganic ions. This complex molecular mixture is animated by both thermally driven diffusion and metabolism, which plays a key role in maintaining the cell interior in a fluid state.[38]

In this crowded, jostling environment, water serves as both solvent and metabolite. Water is obtained from the environment, but a significant fraction of cytosolic water can be generated by microbial catabolism, at least during rapid growth.[39] One major function of this aqueous phase is the solvation of macromolecules, metabolites, and ions.[40] Depending on environmental osmolarity, the portion of cellular water engaged directly in hydrating macromolecules can vary from ∼30% to upward of 90%, with the remaining water serving as lubricant and solvent. At high external osmolarity, this more

https://doi.org/10.1021/acs.biochem.4c00726
Biochemistry 2025, 64, 329−345

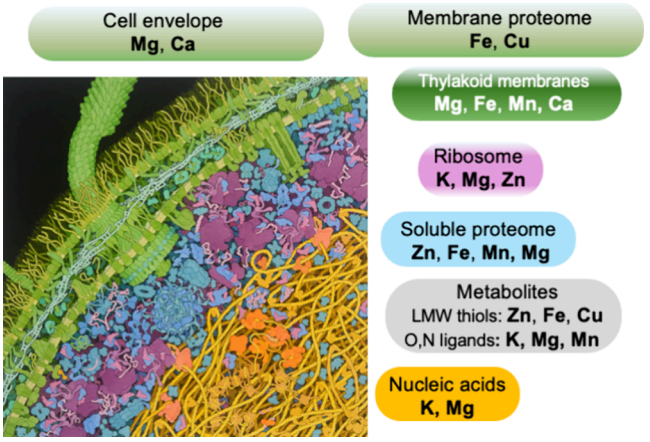

Figure 3. Partitioning of metal ions among bacterial cell constituents. The image is Goodsell's watercolor rendition of a corner of an *Escherichia coli* cell (2021 update).[33] From the upper left, the major structures are the outer membrane with lipopolysaccharide, the periplasm with a thin peptidoglycan layer, and inner (plasma) membrane with embedded membrane proteins. These cell envelope layers also harbor a flagellum. The cytosol contains abundant ribosomes (purple) and soluble proteins (blue), with the most central part of the cell filled by the nucleoid and associated proteins (orange). For each cell compartment, the most dominant cations are indicated on the right. Illustration by David S. Goodsell, RCSB Protein Data Bank. DOI: 10.2210/rcsb_pdb/goodsell-gallery-028 (CC-BY-4.0 license).

mobile water phase becomes depleted and the cytosol transitions to an immobile, glass-like state unable to support metabolic activity. Studies in *E. coli* have correlated the cessation of growth at extremes of high osmolarity with the loss of the mobile water phase.[37] The challenge we face is to understand how metal ions behave in this molecularly crowded and chemically complex environment, with a variable water activity often much less than in dilute solutions.

POTASSIUM AND CELLULAR OSMOTIC BALANCE

On balance, the macromolecular constituents of the cell carry a large net negative charge.[36,41] The single greatest contribution is from the phosphoryl groups of nucleic acids. In *E. coli*, the total concentration of anionic phosphodiester linkages in RNA and DNA is ~330 mM under isosmotic conditions.[36] Cytosolic proteins also contribute with ~63% of *E. coli* proteins predicted to carry a net negative charge at near neutral pH.[42] The metabolite pool is also dominated by anions, with glutamate levels approaching 100 mM and substantial contributions from NTPs and other phosphorylated compounds.[43] These bulk anions prominently feature oxygen atoms that can partially displace water as an inner sphere ligand for K^+ and Mg^{2+}. These two low affinity ions play major roles in charge neutralization of the anionic cell envelope, nucleic acids and ribosomes, and metabolites (Figure 3). The central role of K^+ and Mg^{2+} as bulk ions, and of Mg^{2+} in enzyme catalysis, places these two elements among the dozen or so that are universally essential for life.[9,44]

Potassium ion (K^+) is the second most abundant component in many bacteria (after water, which is ~30−40 M) with concentrations of ~200−800 mM (Figure 2), depending on external osmotic strength.[36,45] This dominant cation maintains osmotic balance[7,46,47] and is an important contributor to the membrane potential.[48] K^+ is hydrated with 6−8 or more loosely bound water molecules that exchange rapidly (picosecond time scale) and the hydrated K^+ ions form both inner and outer sphere ion pairs with cellular anions (Figure 4). Intracellular K^+ pools are buffered by small anions such as glutamate and other

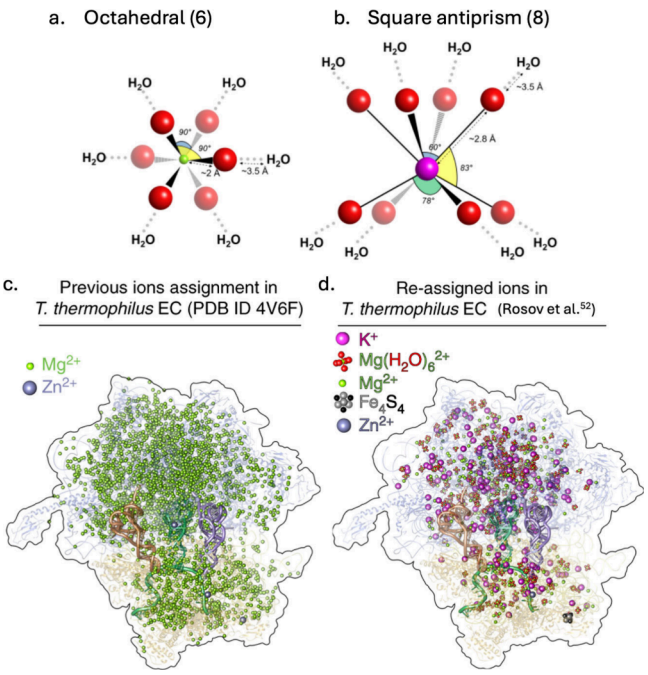

Figure 4. Bulk ions (K^+, Mg^{2+}) are buffered by interactions with ribosomes and other abundant cellular components. The smaller Mg^{2+} ion (green; radius ~0.72 Å) typically has 6 oxygen (red) ligands (a), whereas the larger K^+ ion (magenta; radius ~1.5 Å) has more variable coordination, with 8 ligands common (b). The structure of the 70S ribosome from *Thermus thermophilus* (PDB 4 V6F)[51] has >3000 modeled cations (c). All but 3 of these were initially assigned as Mg^{2+}. A reinvestigation of this structure led to a reassignment of the cations (d). The revised model includes 334 Mg^{2+}, 251 $Mg(H_2O)_6^{2+}$, 1 Zn_2^+ and 1 Fe_4S_4 cluster. Note that the crystallization conditions in both studies contained at least 100 mM KSCN and no added Mg^{2+} ions. Figure adapted from Rozov et al.[52] (CC-BY-4.0 license).

organic acids. The fraction of the K^+ quota that is free or associated with low molecular weight (LMW) ligands has been empirically defined as those ions released from cells when the membrane is transiently permeabilized by hypoosmotic shock.[49] In *E. coli* approximately half (~230 mM) of cytosolic K^+ was found to be bound and the other half (~250 mM) present in the released pool.[50]

The bound K^+ pools are diverse and dynamic, and likely dominated by interactions with ribosomes and nucleic acids. Ribosomal RNA is the single most abundant RNA in the cell, and both K^+ and Mg^{2+} are essential for ribosome function.[53] Stereochemical considerations argue that many sites assigned as Mg^{2+} (Figure 4c) may be occupied instead by K^+ (Figure 4d).[52,54] Ribosome-bound K^+ is coordinated by oxygen (from phosphodiester linkages, carbonyl groups, ribosomal proteins, and water) and nitrogen from the nucleobases.[55] With ~3×10^4 ribosomes per fL (10^{-15} liters) of cell volume,[56] and up to ~400 K^+ site-specifically bound per ribosome,[54] ribosomes may bind up to ~1.2×10^7 K^+ ions (~10% of the cell quota) in these sites alone. This corresponds to ~20 mM K^+ based on an average volume for *E. coli* of 1 fL and the resultant conversion: one atom (or molecule) per cell is ~1.7 nM. A subset of ribosomally associated K^+ is thought to be localized deep within the macromolecular structure where residence times may approach

https://doi.org/10.1021/acs.biochem.4c00726
Biochemistry 2025, 64, 329−345

the lifetime of the folded ribosomal subunits.[54] The dynamics of K^+ in such sites have not been well-defined. Conceptually, we can anticipate that surface-associated K^+ ions are labile, whereas those at the subunit interfaces may be sequestered during translation cycle and then labile when the subunits dissociate, and others deeper within the subunit structures may be sequestered on a longer time scale. Overall, it is likely that nucleic acids and abundant anionic metabolites play the major role in buffering a highly mobile pool of intracellular K^+.

A smaller subset of the bound K^+ pool includes those enzymes that require K^+ for function.[57] K^+-dependent enzymes typically engage the ion through 4 to 8 bonds, which are nearly all to oxygen atoms (Asp, Glu, Ser, Thr).[58] For those enzymes that bind K^+ with the highest affinity (type I enzymes), K^+ is considered a cofactor. For example, propanediol dehydratase is activated by K^+ with a K_M of 0.6 mM,[59] well below the level of the free K^+ pool. However, even these monovalent-activated enzymes are likely part of the labile pool based on predicted dissociation rates. If the K_M of 0.6 mM is a good proxy for the binding constant (K_d), and we postulate a reversible, diffusion-limited binding reaction ($k_a \sim 10^9\ M^{-1}\ s^{-1}$), we can estimate a maximal dissociation rate (k_{off}) of $6 \times 10^5\ s^{-1}$ (where $k_{off} = K_d \times k_{on}$), corresponding to half-life of ~1 ms. Thus, even if the association rate (k_{on}) is orders of magnitude slower, K^+ exchange will occur on a time scale of seconds.

In sum, K^+ is the single most abundant ion in the cell with large and rapidly exchanging pools of free (hydrated) ions and labile complexes with both macromolecules (e.g., nucleic acids, proteins) and metabolites. Importantly, except for K^+ buried within the ribosome, K^+ pools are highly dynamic and exchange rapidly. More broadly, the only widespread mechanism in biology for the partitioning of K^+ (and related Na^+) ions into a "stored" form requires membrane partitioning. For example, in animal cells, the sodium–potassium ATPase maintains transmembrane gradients that serve in secondary active transport and nerve conduction.

MAGNESIUM BUFFERING BY RIBOSOMES AND METABOLITES

Mg^{2+} is the most abundant divalent cation in cells (quota ~100 mM) and plays a central role in nucleic acid structure and as an enzyme cofactor.[5] Cell envelope-associated Mg^{2+} serves as a counterion for membrane phospholipids and lipopolysaccharides in Gram-negative bacteria and this can account for 1/3 of the quota (Figure 3).[60] Similarly, the thick cell walls of Gram-positive bacteria have an enormous ion-binding capacity,[61] with near equal contributions from peptidoglycan and teichoic acids.[62] Here, we focus on the intracellular Mg^{2+} pool (~50–100 mM), which is distributed about equally between a large, macromolecule-associated pool and a LMW pool.[60] Similar to K^+, the bound Mg^{2+} pool of *E. coli* was initially defined as that portion that does not "wash out" of cells permeabilized with EDTA, and this ranges from 1/3 of the total in exponentially growing cells to the majority in Mg^{2+}-starved cells.[63]

Mg^{2+} functions in the charge neutralization and folding of many nucleic acids, with the ribosome again serving as a major reservoir.[64] A comprehensive analysis of $>10^4$ Mg^{2+} binding sites in RNA-containing structures reveals that ~1/3 of Mg^{2+} ions retain only water as inner sphere ligands.[65] Similarly, in ribosome structures from the protein database (PDB) over 20% of Mg^{2+} is fully hydrated with only outer-sphere coordination to the ribosome.[65] In the ribosome, just over half of ions assigned as Mg^{2+} retain four or more water molecules as ligands, with the most common RNA-associated, inner sphere ligands being the nonbridging oxygen atoms from the phosphate backbone.[65] Both Mg^{2+} and K^+ therefore function in charge neutralization as mobile, outer-sphere ions, with Mg^{2+} favored at sites of unusually high negative charge density.[66]

The ribosome is the most abundant macromolecule in the cell, and both K^+ and Mg^{2+} are required for function. However, determining the number and location of ribosome-associated ions has been challenging (Figure 4). The number of assigned Mg^{2+} ions varies widely, but in most cases Mg^{2+} is only sufficient to neutralize a fraction of the RNA charge,[65] with the rest neutralized by ribosomal proteins and other cations. As an upper limit, > 3000 cation-binding sites were visualized in the *Thermus thermophilus* 70S ribosome[51] and assigned as Mg^{2+}, but those assignments have been challenged on both experimental[52] and stereochemical[54] grounds. Long-wavelength X-ray crystallography suggested a total of ~600 Mg^{2+} with 334 having inner-sphere coordination and 251 outer sphere coordination[52] (Figure 4). Further analysis using stereochemical constraints refined these estimates further and assigned ~400 monovalent ions and ~100 Mg^{2+} in the first solvation shell.[54] Of note, these values are based on analyses of ribosomes crystallized from a solution high in K^+ (100 to 200 mM KSCN) and lacking Mg^{2+}.

Ribosome structures can now be determined to better than 2 Å resolution using cryo-electron microscopy (cryo-EM).[67] In the *E. coli* 70S ribosome, 309 Mg^{2+} and 2 Zn^{2+} ions were assigned by this method, but K^+ was not included in the solvent and was not assigned.[67] If we take ~300 as a reasonable estimate for the number of Mg^{2+} tightly associated with the ribosome this can account for ~15–20 mM of the overall ~100 mM Mg^{2+} quota. Other estimates of the contribution of the ribosome to Mg^{2+} pools are in this same range, corresponding to ~12 mM in *E. coli*[5] or as much as ~25% of the quota.[60] Since even the inner sphere coordination sites often involve only 2 to 3 ligands from the ribosome, it is possible that many of these sites can accommodate either Mg^{2+} or K^+, depending on the ambient levels in the cell. Since cryo-EM approaches are more amenable to the use of biologically relevant buffer conditions and metal concentrations, it will be interesting to test this hypothesis experimentally. However, accurate metal assignments are not trivial, and even structures determined by X-ray crystallography (where anomalous scattering can provide relevant information) have had metals assigned incorrectly.[68] As an alternative approach to infer the lability of ribosome-bound Mg^{2+} ions, a coarse-grained elastic network model has been used to identify those sites with the greatest dynamic flexibility as candidates for the most labile cation binding sites.[69] In sum, the ribosome acts as a site of counterion condensation that buffers both K^+ and Mg^{2+}, and possibly other ions.[70] We still have a poor understanding of which sites are truly specific for one ion, and whether the exchange kinetics of any sites are sufficiently slow to allow sequestration of metal ions.

Collectively, ribosomes and other negatively charged macromolecules and metabolites buffer free Mg^{2+} near 1 mM, with a range of ~0.3 to 3 mM.[5,8,71,72] The LMW Mg^{2+} pool is dominated by ATP and other NTPs[60] that bind Mg^{2+} with relatively high affinity (K_d values of ~0.1–0.3 mM).[43] Consistent with these estimates, the essential *Bacillus subtilis* MgtE Mg^{2+} importer, a homologue of the solute carrier family 41 (SLC41) proteins in human,[73] is regulated by a Mg^{2+}-sensing riboswitch[29] with half-maximal repression at 2.7 mM free Mg^{2+}. MgtE functions as a Mg^{2+}-gated channel and is also feedback inhibited when intracellular Mg^{2+} reaches ~4 mM and binds to

https://doi.org/10.1021/acs.biochem.4c00726
Biochemistry 2025, 64, 329–345

several cytoplasmic sensing sites.[74,75] These concentrations thereby serve as a signal of Mg^{2+} sufficiency and reveal the homeostatic set-point for free Mg^{2+} (Figure 2). A free pool in the low mM range is also consistent with the observed requirement for Mg in both enzyme and RNA-dependent catalysis. For example, *B. subtilis* RNase P binds ∼150 Mg^{2+} ions with an apparent affinity ($K_{1/2}$) of 0.26 mM Mg at low K^+ (∼50 mM K^+), decreasing to a $K_{1/2}$ of ∼1.5 mM Mg^{2+} with higher K^+ (∼150 mM K^+).[76] Thus, free Mg^{2+} levels in the low mM range are just sufficient to sustain RNase P activity.

The large pools of K^+ and Mg^{2+} associated with ribosomes (Figure 4), other nucleic acids, and metabolites overlap in their binding sites, which can lead to interesting physiological consequences. In *B. subtilis*, hyperosmotic shock leads to a large accumulation of intracellular K^+ (≥700 mM), which mobilizes Mg^{2+} ions.[77] These displaced Mg^{2+} ions are exported from the cell, and the Mg^{2+}-limited cell is unable to sustain translation. Cells adapt to the stress of osmotic shock through the synthesis or import of compatible solutes and growth resumes after a substantial lag. The resumption of growth is driven by the reimport of sufficient Mg^{2+} to allow a resumption of translation.[77]

Since Mg^{2+} association with nucleic acids and metabolites is very dynamic, the identity of any nonlabile (sequestered) pools of Mg^{2+} is not clear. One possibility is Mg^{2+} bound within the ribosome, or to other large RNA molecules, at sites that are not available for exchange with solvent. One common mechanism for Mg^{2+} storage is membrane-bound vacuoles, as seen in *S. cerevisiae* and higher plants,[78] but this mechanism has not been documented in bacteria. Another candidate is Mg^{2+}-dependent enzymes. Although many Mg^{2+}-dependent enzymes bind to ATP:Mg^{2+} (or other substrate:Mg^{2+} complexes), a subset form relatively stable associations with Mg^{2+} (K_d of 10−100 μM),[71] and it is possible that some of this Mg^{2+} may be functionally sequestered. DNA and RNA polymerases function with multiple Mg^{2+} ions in their active site,[79] with the highest affinity binding having a K_d of ∼50−100 μM.[80] The role of Mg^{2+} in these and related enzymes can be substituted by other divalent metal ions with variable efficacy.[80] Similarly, enzymes of the menaquinone, siderophore, and tryptophan (MST) family bind Mg^{2+} reversibly with a K_d of ∼0.2 mM.[81] This Mg^{2+} can be readily displaced by Fe^{2+} or Mn^{2+} leading to enzyme inhibition,[81,82] suggesting that this Mg^{2+} is labile.

Overall, the high propensity of Mg^{2+} to retain water ligands during transient association with macromolecules or metabolites suggests that there may be relatively little Mg^{2+} that is truly sequestered. One notable exception is photosynthetic organisms, which can have high levels of chlorophyll, a Mg^{2+}-porphyrin complex, sequestered within large, membrane-associated photosynthetic complexes (Figure 5). In cyanobacteria, chlorophyll-associated Mg^{2+} pools may be as high as ∼25 mM.[83] The insertion of Mg^{2+} into protoporphyin IX requires an exchange of preferred O ligands (e.g., water) with less preferred N ligands from the porphyrin macrocycle. The reaction catalyzed by Mg^{2+} chelatase is unfavorable ($K_{eq} \sim 10^{-6}$) and is coupled to ATP hydrolysis.[84] Once synthesized, chlorophyll-Mg complexes are stable (spontaneous Mg^{2+} loss occurs with a half-time of ∼6 h),[84] and therefore no longer part of the labile pool. However, it is unlikely that evolution has ignored this valuable pool of sequestered Mg^{2+}. One of the classical mutations used by Gregor Mendel during his studies of inheritance leads to a "stay-green" phenotype in pea seed cotyledons and encodes a Mg^{2+}-dechelatase that converts chlorophyll to pheophytin by removal

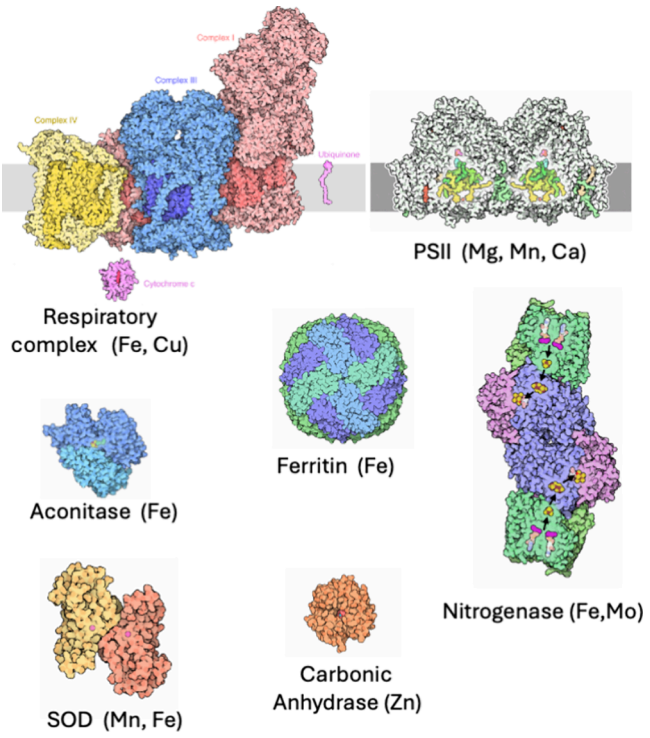

Figure 5. A gallery of metalloproteins that contribute to intracellular sequestered, conditionally sequestered, and labile metal pools. The large respiratory complex (motm/273) contains abundant iron and is a major destination for copper. In cyanobacteria and other phototrophs, intracellular membranes contain abundant chlorophyll molecules (Mg), and PSII additionally contains the Mn,Ca-containing oxygen-evolving complex (motm/59). Nitrogenases are rich in iron and molybdenum (motm/26). Metals in these large complexes are generally considered to be sequestered. Ferritins (motm/35) are hollow, spherical molecules with 24 identical subunits that oxidize and store iron in their hollow interior. This sequestered iron is conditionally mobilized in response to iron deprivation. Aconitase (motm/89) contains a 4Fe4S cluster that can reversibly lose iron in response to oxidative stress or iron depletion. Bacterial cytosolic superoxide dismutases (SOD; motm/94) are activated by reversible binding of manganese or iron (or both). MnSOD contributes a significant fraction of the cytosolic Mn^{2+} pool. Carbonic anhydrase (motm/49) is a zinc-dependent enzyme that binds Zn^{2+} tightly.[109] All illustrations were drawn by David S. Goodsell for the RCSB PDB as part of the ongoing PDB-101 molecule of the month (motm) feature[110,111] accessible at: https://pdb101.rcsb.org/motm/XY (where XY refers to the numbers noted above) and are not all presented at the same scale. Images are reproduced under a CC-BY-4.0 license.

of the central Mg atom.[85] This enzyme is postulated to help mobilize Mg^{2+} during Mg^{2+} limitation in plants.[86] Although homologues are present in some nonphotosynthetic Bacteria and Archaea,[87,88] they are lacking in the cyanobacteria. Whether bacteria contain mechanisms to recover Mg^{2+} from photosynthetic complexes in Mg^{2+}-starved cells is unclear.

MANGANESE: METALLOPROTEINS, RESERVOIRS, AND OXIDATIVE STRESS

Manganese (Mn) and iron (Fe) have a moderate affinity for ligands, as seen in the Irving-Williams series. Although both are critical nutrients for most bacteria, the cellular quotas for these metals are variable and typically <1 mM,[11] a value ∼100-fold lower than K^+ and Mg^{2+} (≥100 mM). Some bacteria are iron-centric with relatively large iron quotas and a much lower, and

https://doi.org/10.1021/acs.biochem.4c00726
Biochemistry 2025, 64, 329−345

sometimes conditional, demand for manganese (Figure 2). *E. coli* falls in this category and Mn^{2+} import is specifically induced as a response to oxidative stress.[89,90] Other organisms, such as *B. subtilis*, have a more balanced demand for manganese and iron.[10,91] A few organisms seem to have dispensed with an iron requirement altogether, including the lactic acid bacteria[92,93] and the pathogenic spirochete *Borrelia burgdorferi*.[94] Growth in the absence of iron imposes considerable metabolic restrictions, including a lack of respiratory chains and other heme-containing enzymes. The bulk of the quota for manganese and iron is devoted to intracellular enzymes (Figure 3), with a variable fraction partitioned to the membrane (e.g., respiratory complexes) or to extracellular enzymes. The latter may require dedicated pathways for their maturation.[95,96]

Manganese (Mn) is a critical element for most forms of life, although levels of manganese are exceedingly low in some bacteria.[97] The overall manganese quota varies widely, with the ratio of Mn:Fe ratio varying by >6 orders of magnitude.[97] Intracellular manganese is often bound to specific metalloenzymes, including mononuclear manganese enzymes and those with more complex arrangements that may involve other metals. Bound manganese can serve as an electrophilic center or in redox reactions. Of note, manganese is essential for the oxygen-evolving complex of photosystem II that is the defining feature of oxygenic photosynthesis.[98] Manganese is therefore a critical nutrient for cyanobacteria,[99] algae, and plants and is ultimately responsible for the oxygenation of Earth's atmosphere.[100]

Our current best estimates of the labile manganese pool in model bacteria derive from measurements of the amount of free Mn^{2+} required for regulation of gene expression by Mn^{2+}-dependent regulators such as the MntR transcription factor[101,102] and Mn^{2+}-dependent riboswitches.[103] These analyses suggest that free Mn^{2+} in the 3 to 6 μM range represents sufficiency (Figure 2), and levels approaching 10 μM represent excess.[102] Since the total manganese quota in these same cells is on the order of 500 μM we can infer that most manganese is bound to, and buffered by, macromolecules and metabolites. The precise distribution of manganese between proteins, other macromolecules, and metabolites is still poorly resolved, even in the best studied model systems. In *Bacillus anthracis*, the manganese metalloproteome is dominated by a single enzyme, the manganese superoxide dismutase (MnSOD).[104] This abundant protein is present in up to 30,000 copies per cell in *B. subtilis*,[105] representing up to 50 μM Mn (~10% of the quota). Similarly, in the highly radiation resistant Gram-negative bacterium *Deinococcus radiodurans*, MnSOD can account for 40% of intracellular manganese.[106] MnSOD (Figure 5) represents an abundant pool of Mn^{2+} that may be redistributed to support essential manganese-dependent enzymes during starvation. Consistently, cells lacking MnSOD (which is dispensable) are compromised in growth when transferred to Mn-limiting media.[107] MnSOD can also be metalated by iron, although this can lead to reduced activity and thereby increase cell sensitivity to oxidative stress.[108]

Manganese coordination environments in cells have been probed using electron paramagnetic resonance (EPR)-based techniques that take advantage of the fact that Mn^{2+} is high-spin with a unique EPR signature.[112,113] In cells treated with a cell permeable siderophore, deferoxamine, labile Mn^{2+} pools are stabilized as an EPR-silent Mn^{3+} complex. Quantitation of this quenching suggests that roughly one-half of intracellular Mn^{2+} is in a labile pool accessible to deferoxamine.[112] The EPR signals from intracellular Mn^{2+} complexes reveal that, on average, the 6 to 7 coordination sites are occupied by ~3 to 4.5 water molecules and ~0.5 to 1.5 N atoms, with most of the remaining ligands from phosphates (inorganic phosphate, phosphorylated metabolites, and nucleic acids), with a negligible contribution from carboxylates.[113] Given the high abundance of ribosomes in bacterial cells, it is reasonable to suggest that some of this Mn^{2+} is ribosome-associated. Indeed, *E. coli* ribosomes can bind up to 500 Mn^{2+} ions and are still active in translation.[70] Similarly, ribosomes can bind >500 Fe^{2+} ions, although these ribosomes were less functional than those reconstituted with Mn^{2+}. These results suggest that the repertoire of ribosome-associated cations may be variable in cells, and that the ribosome may serve as a general cation buffer.[70]

Manganese homeostasis has been studied in detail in *D. radiodurans*.[114,115] This bacterium, notable for its exceptionally high resistance to ionizing radiation, has a high manganese quota (up to 4 mM) and an exceptionally high Mn/Fe ratio (0.24).[116] Manganese accumulates bound to inorganic phosphate and phosphorylated metabolites (e.g., fructose-bisphosphate), small peptides, and nucleosides.[106,116] A subset of these complexes (e.g., Mn:P_i) endow the cell with a nonenzymatic mechanism to detoxify reactive oxygen species and thereby protect against oxidative damage.[115] The presence of substantial cytosolic pools of Mn^{2+} in complex with phosphate and other low molecular weight ligands is also observed in the model yeast *Saccharomyces cerevisiae*.[117] In this organism, elevated intracellular Mn^{2+} can suppress growth defects arising from the absence of SOD.

IRON: ENZYMES, COFACTORS, STORAGE, AND SPARING

Iron (Fe) is almost universally essential for life and is among the most fiercely fought over elements.[118,119] Iron is redox active, and very poorly soluble in the oxidized Fe^{3+} (ferric) form, which has led to the evolution of high affinity iron-binding compounds (siderophores) synthesized by many bacteria and fungi.[18,19] Since the uptake of ferric-siderophores requires specific transporters, competition for iron begins extracellularly and cheating is common. In human physiology, sequestration of iron is a central feature of nutritional immunity,[120] and pathogens have evolved a wide variety of mechanisms to liberate iron from host stores.[121]

The iron quotas in the model organisms *E. coli* and *B. subtilis* are ~500 μM, which is predominantly in the reduced Fe^{2+} (ferrous) state.[122−124] The majority of this iron is bound to enzymes, including those using FeS clusters or heme as cofactors.[125] When grown with an abundance of iron, the cell may sequester iron in hollow multimeric proteins (ferritin,[126,127] mini-ferritins,[128] and bacterioferritins[129]) (Figure 5). These stored iron pools are in the form of ferric-hydroxide and ferric-hydroxyphosphate complexes and can be monitored using Mössbauer spectroscopy.[130,131] Mobilization of these stored iron pools often requires reduction,[132] or in some cases proteolysis,[127,133] and occurs on a time-scale of minutes. Iron may also be stored by loading into dedicated membrane-bound organelles known as ferrosomes,[134,135] but their biology is only beginning to be understood. In many bacteria, homeostasis also relies on Fe^{2+} export,[136,137] particularly under conditions of high Fe^{2+} and oxidative stress.[138−140]

The free and labile iron pools account for a small fraction of the iron quota. The best estimates of the free Fe^{2+} pool are on the order of <1 μM.[4] The ferric uptake repressor (Fur; Figure 2) binds Fe^{2+} with an affinity (K_d) of 1.2 μM in *E. coli*[141] and 0.8 μM

https://doi.org/10.1021/acs.biochem.4c00726
Biochemistry 2025, 64, 329−345

in *B. subtilis*, and even lower levels suffice to stabilize DNA-binding due to the additional coupling free energy.[101] The labile iron pools additionally include iron that is chelated weakly and is therefore exchangeable. This labile pool has been estimated as ~10 μM Fe^{2+} using a cell-permeable iron chelator (desferrioxamine) that can convert labile Fe^{2+} into an EPR-detectable ferric complex.[123] However, this value increases to ~80 μM in cells growing aerobically and lacking superoxide dismutase (SOD).[123] A similar value of ~80 μM for the labile pool was reported based on the ultrafiltration of *E. coli* lysates.[142]

The molecular composition of the labile iron pool has been a topic of active debate. Among metabolites, the abundant LMW thiol glutathione (GSH; L-γ-glutamyl-L-cysteinyl-glycine) binds Fe^{2+} with sufficient affinity to form part of the buffered pool.[143] However, recent studies using Mössbauer spectroscopy of anaerobically generated *E. coli* lysates have defined a low molecular mass, labile pool dominated by Fe^{2+} complexes with NTPs and citrate, and GSH complexes were not detected.[124] However, GSH likely plays a role in iron mobility, at least transiently. For example, in mammals GSH-Fe^{2+} complexes interact with iron chaperones (PCBP proteins) important for the distribution of iron to storage proteins (ferritin), nonheme iron enzymes, and the ferroportin (Fpn1) iron exporter.[144] Low molecular thiols are also implicated in iron-trafficking in organisms that do not use GSH as their major thiol. In *B. subtilis*, bacillithiol (BSH)[145] is important for the synthesis of FeS proteins.[146,147] Proteins may also play a role in iron buffering. Some iron-binding enzymes behave more as iron-activated enzymes rather than stable metalloproteins,[148] and Fur is unusually abundant for a regulator and could also function as an Fe^{2+}-buffering protein.[101]

The majority (>80%) of the iron quota is partitioned into the metalloproteome, although the composition and lability of this pool is highly variable even within a single organism. Much of this iron may be sequestered in the form of heme in abundant enzymes (e.g., catalase) and in respiratory chain components (Figure 5). Dysregulation of iron partitioning has serious consequence for cell physiology. For example, the PerR regulator normally binds DNA in association with either Mn^{2+} or Fe^{2+}, and PerR:Fe^{2+} reacts with hydrogen peroxide to derepress oxidative stress genes.[149,150] Oxidation of *B. subtilis* PerR normally leads to the transient expression of genes encoding an abundant cytosolic catalase and for synthesis of the required heme cofactor,[151,152] followed by a reestablishment of repression by newly synthesized PerR protein.[153] However, in *perR* null mutants the constitutive expression of heme biosynthesis and catalase depletes iron pools and cells grow poorly unless high levels of supplemental iron are added.[122] Conversely, mismetalation of PerR with Zn^{2+} leads to a dyscoordination of expression wherein heme biosynthesis genes are derepressed, while the gene for catalase (the major heme sink) is still repressed. As a result, heme is produced in excess and partitions to the membrane where it leads to redox stress.[154] In general, excess heme generates reactive oxygen species, likely by reaction with membrane-localized quinols.[155] As protection, cells may induce specific heme exporters or heme sequestration proteins.[156]

In addition to heme enzymes, the iron−metalloproteome includes enzymes with FeS clusters and those with a single bound iron cofactor (mononuclear Fe enzymes). A subset of this bound iron can be mobilized under conditions of oxidative stress: elevated superoxide liberates iron from some solvent-exposed Fe_4S_4 clusters, and hydrogen peroxide oxidizes and releases iron from some mononuclear iron enzymes.[157] These pools of sequestered iron are substantial and their mobilization can elevate the labile iron pool by several-fold.[123] The spontaneous dissociation of iron from selected mononuclear enzymes has been estimated to occur with a half-life on the order of an hour, which is comparable the doubling time of the cell.[91] However, a subset of this iron pool is readily mobilized under conditions of metal ion imbalance including, for example, Zn^{2+} intoxication.[3,158]

The amount of iron sequestered in enzyme complexes can be significant, and when iron is limited, cells act to minimize this pool. Iron-sparing responses, often mediated by translational repression mediated by small RNAs, have been defined in many bacteria.[159] These systems transiently repress the synthesis of selected FeS-containing proteins and heme enzymes to allow limited iron to be directed to the highest priority enzymes.[159−161] The extent to which cells actively degrade iron-containing proteins and protein complexes to redeploy the metal is less clear. One striking example is in the marine diazotroph *Crocosphaera watsonii*. This organism reduces its cellular iron quota by 40% by synthesizing iron-rich photosynthetic complexes during the day, and then degrading these each night to redeploy the iron for synthesis of nitrogenase.[162] Although protein degradation and synthesis is energetically costly, this photoautotroph can readily obtain energy by photophosphorylation, and both carbon and nitrogen are obtained directly from the atmosphere: it is iron that would otherwise limit growth.

In sum, manganese and iron are largely partitioned into the proteome while also maintaining a substantial labile metal pool. Based on their binding affinity and kinetic properties, many manganese enzymes are likely to be in equilibrium with the free Mn^{2+} pool (estimated at $>10^3$ aquated Mn^{2+} per cell), thereby providing a mechanism for Mn^{2+} partitioning to adapt dynamically to cellular needs based on the synthesis of new apoproteins (Figure 1). In the ambient conditions of the cytosol, iron is mostly Fe^{2+}. Iron is dynamically partitioned between mononuclear iron proteins, FeS-containing enzymes, and heme proteins, but the corresponding regulatory mechanisms are incompletely understood. A significant subset of iron enzymes bind iron reversibly, or are susceptible to oxidation, and these may therefore contribute to the labile pool. Metal ion competition and the effects of mismetalation further complicate the situation.[158,163]

■ ZINC: METALLOPROTEINS AND INTRACELLULAR RESERVOIRS

There is a stark contrast between the high affinity metal ions, zinc (Zn^{2+}) and copper ($Cu^{2+/+}$), and the low affinity bulk ions, K^+ and Mg^{2+}. Unlike the latter, cells have lower quotas for zinc and copper, with the vast majority sequestered in protein complexes, and there are no free ions present at equilibrium. As elements from the high affinity end of the Irving-Williams series, both Zn^{2+} and Cu^+ (the predominant form in the cytosol) bind ligands tightly and their movement within cells is facilitated by ligand exchange reactions.

The Zn^{2+} quota in microbial cells is substantial and variable, with concentrations often in the same range as for manganese and iron (Figure 2). For *E. coli*, the Zn^{2+} quota is ≥100 μM, and this value increases up to 5-fold after a Zn^{2+} shock.[164] In the marine cyanobacterium *Synechococcus*, induction of a Zn^{2+}-storing metallothionein allows quotas to vary over a 50-fold range.[165] Similarly, in *Cupriavidus metallidurans*, a Gram-

https://doi.org/10.1021/acs.biochem.4c00726
Biochemistry 2025, 64, 329−345

negative β-proteobacterium isolated from environments with high levels of metals, the Zn^{2+} quota varies by >10-fold and can approach 1 mM.[166] In *B. subtilis*, ~500 μM Zn^{2+} is present under replete conditions, and this increases to >2 mM in response to a Zn^{2+} shock.[167]

As a high affinity ion, Zn^{2+} binds much more strongly to many biomolecules than to water, and at equilibrium there are no free Zn^{2+} in the bacterial cytosol.[24] Instead, the labile Zn^{2+} pool is buffered by the reversible binding of Zn^{2+} to metabolites, exchangeable sites in proteins, and to metallochaperones. Zn^{2+} bound to small molecule ligands, including LMW thiols and other sulfur- and nitrogen-containing metabolites, exchanges rapidly and is part of the labile pool. Recent estimates place the *E. coli* Zn^{2+} quota at 200 ± 100 μM in the soluble, cytosolic fraction, with a small subset (~13 μM) in a low-molecular mass pool as judged by ultrafiltration.[142] This labile pool can increase dramatically in response to a sudden influx of Zn^{2+}.[167] Zn^{2+} homeostasis is regulated to ensure that the Zn^{2+} metalloproteome is appropriately metalated and that excess Zn^{2+} is either well-buffered or exported from the cell to help avoid mismetalation of enzymes that normally use other metal cofactors.[168] *C. metallidurans* accumulates ~10^5 ions per cell under replete conditions, and this value is similar in magnitude to the estimated total number of Zn^{2+}-binding sites in the proteome.[166] Similarly, the much larger cells of the yeast *Saccharomyces cerevisiae* have Zn^{2+} quotas ranging from 2×10^5 to 2×10^6 atoms per cell, with an estimated Zn^{2+}-binding capacity in the proteome of ~10^5 atoms.[169] Collectively, these results suggest that the Zn^{2+} metalloproteome accounts for much of the Zn^{2+} quota under replete conditions, but this pool may be undersaturated when Zn^{2+} is limited.

The Zn^{2+} metalloproteome is generally considered to be sequestered on the time scale of cell growth and division, although there are a wide range of dissociation rates and some sites may be labile, at least under some circumstances.[170] Zinc coordination most commonly involves Cys, His, or carboxylate-containing residues with 3 ligands (and water) in many Zn^{2+} enzymes, and 4 tetrahedral ligands for structural Zn^{2+}. Bound Zn^{2+} dissociates very slowly *in vitro* with, for example, a k_{off} for human carbonic anhydrase II of 0.0003 h^{-1} (a half-time of ~3 months).[170] However, exchange may occur more rapidly in the cellular context if ligands, such as LMW thiols, can access the zinc to facilitate release through a ligand exchange mechanism. Even ligands that are themselves too weak to outcompete a protein for Zn^{2+} can transiently mobilize Zn^{2+} to a form that can then be sequestered by higher affinity chelators. This effect, dubbed catalytic chelation, is likely important in the cellular milieu.[170,171] For example, the metalloenzyme ribulose-5-phosphate 3-epimerase binds Zn^{2+} as a competitive inhibitor for the preferred Fe^{2+} cofactor, and spontaneous Zn^{2+} dissociation occurs with a half-time of ~8 h.[172] However, in cells Zn^{2+} dissociation and enzyme reactivation occurs with a half-time of ~15 min, which was attributed to a possible role of free cysteine in facilitating ligand exchange.[91,173] In *B. subtilis*, *in vitro* studies reveal that BSH can increase the rate of transfer of Zn^{2+} from the metalloregulator CzrA to the high affinity chelator TPEN, even though BSH alone is unable to remove Zn^{2+}.[167]

Catalytic chelation may also serve to mobilize Zn^{2+} in times of need. In many bacteria, a subset of ribosomal proteins bind Zn^{2+}.[64,174,175] Because of the high abundance of ribosomes, this can represent the single largest Zn^{2+} repository in the cell.[176] When *B. subtilis* cells experience Zn^{2+} deprivation, the earliest response is the mobilization of these Zn^{2+} stores through the synthesis of competing proteins to displace the Zn^{2+} metalloproteins from the surface of the ribosome.[177] Whether the bound Zn^{2+} is then mobilized from these small Zn^{2+} proteins (which are similar in size to a single zinc-finger) by catalytic chelation or through proteolytic degradation is unresolved.[64] Regardless of mechanism, these Zn^{2+}-containing small ribosomal proteins serve as a conditionally sequestered storage form of Zn^{2+}.

Once the Zn^{2+} metalloproteome is saturated, buffering and storage mechanisms become important.[178] In some organisms, excess Zn^{2+} may be stored in metallothioneins, cysteine-rich metalloproteins with a high binding capacity for thiophilic metals.[178] In addition, Zn^{2+} can be buffered by interaction with metabolites, including low molecular weight thiols such as GSH[179] and BSH.[167] Despite the overall high levels of Zn^{2+} in cells, the estimated free Zn^{2+} pool, as judged by the sensitivity of Zn^{2+}-sensing metalloregulators, is in the pM to fM range.[24,27,101,165,180] The implication is that there is no free Zn^{2+} in the cytosol under most conditions. However, free Zn^{2+} pools can increase to ~50 nM after a 50 μM Zn^{2+} shock that saturates the highest affinity Zn^{2+} buffers in the cell, thereby leading to a small and transient pool of free Zn^{2+} ions.[164] Similar labile Zn^{2+} pools are seen in other organisms, including eukaryotes.[181]

Although the level of free Zn^{2+} can vary by several orders of magnitude (from sub-pM to nM), this change can be triggered by relatively small increases in Zn^{2+} levels that saturate the highest affinity ligands and begin to engage lower affinity Zn^{2+} buffers. For example, in *B. subtilis* the major LMW thiol is BSH, which is present at mM levels and serves as an important Zn^{2+} buffer.[182−184] Under conditions of Zn^{2+} sufficiency, only a small fraction of the BSH pool is bound to Zn^{2+} ion.[167] Measurement of the affinity of BSH for Zn^{2+} reveals that if an intracellular pool of 1 mM BSH were 1% saturated with Zn^{2+} (yielding 5 μM BSH_2:Zn^{2+}), Zn^{2+} would be buffered to 2.5 pM. Conversely, exposing cells to a Zn^{2+} shock (0.25 mM Zn for 5 min) leads to a ~ 3-fold increase in total Zn^{2+} (from ~0.8 to 2.4 mM), with much of this increase associated with a LMW mass pool that is dependent on BSH.[167] Calculations reveal that 80% saturation of a 1 mM BSH pool would buffer free Zn to ~5 nM, which is more than sufficient to inactivate the CzrA repressor to induce expression of Zn efflux proteins.[167] This example illustrates how a single molecule, BSH, can buffer Zn^{2+} over physiologically relevant concentrations. The actual speciation in cells is undoubtedly more complex. Ongoing efforts to develop chemical probes to track Zn levels and distribution in living cells provide hope that further insights will be forthcoming.[185,186]

COPPER: INTRACELLULAR TRAFFICKING AND STORAGE

Copper (Cu) is a critical metal for many microbes but is required in relatively low levels. Although copper is considered essential for most Eukaryotes, most cells have only a handful of copper-dependent enzymes. For example, in a survey of β-proteobacteria, copper-related proteins typically represent <1% of the proteome, inclusive of cuproenzymes, chaperones, and transporters.[187] In many anaerobes, copper appears to be dispensable.[188] The most common copper-dependent enzymes, found in all three Domains of life, are the copper-dependent terminal oxidases in the respiratory chain. Under conditions of sufficiency, many organisms have a copper quota of ~1−10 μM averaged over the cell volume. For *E. coli*, the copper quota is

https://doi.org/10.1021/acs.biochem.4c00726
Biochemistry 2025, 64, 329−345

~10^4 atoms per cell (~10 μM),[189] and ~5000 atoms per cell is typical for *C. metallidurans*.[190] For *B. subtilis*, a somewhat lower copper quota of ~1000 atoms per cell (~1 μM) has been reported, which can be reduced ~100-fold when uptake is impaired.[191] The copper quota has been well studied in the photosynthetic alga *C. reinhardtii* (with a cell volume 500-fold more than *E. coli*) where replete cells contain ~10^7 atoms (up to 20 μM), with ~20-fold lower levels during Cu-limitation.[192]

Nearly all described copper enzymes in bacteria are membrane-associated or periplasmic. Despite their location, copper-loading often requires copper import from the environment (where it is Cu^{2+} in aerobic environments) into the cytosol where it is reduced to Cu^+, and then export from the cytosol by a dedicated transport system.[31,193] Copper-trafficking requires copper-binding metallochaperones, proteins that collect copper from importers and distribute copper to the transporters and cuproproteins.[194,195] Since copper is trafficked through the cytosol on its way to its ultimate destination the cell must guard against copper toxicity. Due to its high affinity for ligands (as seen by its placement in the Irving-Williams series), copper can displace metals from other metalloenzymes leading to enzyme inhibition.[158] Intracellular copper levels are closely monitored by dedicated metalloregulatory proteins such as CsoR and CueR, and these proteins may detect Cu^+ following transfer from intracellular metallochaperones.[196]

Intracellular trafficking of Cu^+ by chaperones is mediated by ligand exchange reactions between proteins and may also involve LMW thiols as transient ligands. The intracellular Cu^+ pool is buffered to a nominal free Cu^+ level of ~10^{-21} M (zeptomolar) in *E. coli*, as judged by the sensitivity of the CueR metalloregulator for Cu^+.[189] This implies the presence of a very high affinity Cu^+ buffer, presumably a thiol-rich protein. LMW thiols likely play a transient role by catalytic chelation: protecting the cell from copper toxicity and facilitating the ligand exchange reactions to help load metallochaperones. For example, GSH is implicated in Cu^+ trafficking in *Streptococcus pyogenes*,[197] BSH can bind Cu^+ together with the CopZ metallochaperone in *B. subtilis*,[198] and cysteine-copper complexes accumulate in acidocalcisomes in *Chlamydomonas*.[199] However, the affinity of LMW thiols for copper is too low to sustain a sizable and persistent copper pool.[189,200]

The overall picture is one in which there is no free copper in the cell,[201] but there is a small labile pool of Cu^+ that is mobilized through associative, ligand-exchange reactions.[194,195] The primary intracellular Cu^+ depot is likely to be a cysteine-rich protein. In the Eukarya and some bacteria, this role may be filled by metallothionein.[202,203] In methanotrophs, which have a particularly high Cu demand, a family of small multimeric, Cys-rich proteins (copper-storage proteins) were described, including both secreted (Csp1 and Csp2) and cytosolic (Csp3) representatives.[204] Cytosolic Csp3 family proteins are found in a wide range of bacteria and in some Archaea.[204,205] Like metallothioneins, Csp3 proteins can bind Cu^+ in tetranuclear Cu^+-thiolate clusters,[206] with a tetrameric Csp3 protein able to bind at least 70 Cu^+ ions.[207] Although Csp3 proteins bind Cu^+ with high affinity (average $K_d = 5 \times 10^{-18}$ M),[206] these ions can be mobilized by ligand exchange reactions with LMW cellular thiols[196] or by direct transfer to a client protein, as documented for the *B. subtilis* Csp3 protein and a copper-containing laccase expressed in sporulating cells.[208] Copper mobilization and trafficking is likely dictated by mass action and the demand for copper from biosynthetic processes.[31,204] Whether metallothioneins and Csp3 proteins have sufficient avidity to buffer Cu^+ ions to the low levels reported in some systems,[189] or whether they are mostly engaged when there is an excess of Cu^+, is an open question.

The Central Role of Thiols as a Metal Ion Buffer. As this brief review has highlighted, the intracellular mobility of Zn^{2+} and Cu^+ is mediated by the presence of thiol-containing chaperones and high concentrations of LMW thiols. The appreciation of the role of Cu^+ chaperones in trafficking Cu^+ to their client proteins owes an intellectual debt to studies of another thiophilic metal, Hg^{2+}. The extremely high affinity of Hg^{2+} for sulfur-containing ligands is widely known (HgS; $K_{sp} = 2 \times 10^{-53}$), and thiols are also called mercaptans for this reason (from the Latin, *mercurium captans*, meaning mercury-capturing). Like Cu^+, Hg^{2+} binds tightly to Cys, GSH, and other LMW thiols. Despite this extremely high affinity, Hg^{2+} is surprisingly mobile and bacterial cells exposed to Hg^{2+} sense this metal and mount a transcriptional response within minutes.[209]

Insights into how Hg^{2+} could move through cells emerged from studies of its thiolate coordination chemistry using proton NMR: Hg^{2+} forms both 2:1 and 3:1 coordination complexes with GSH that are in equilibrium on a millisecond time scale.[210] This provides a model for how Hg^{2+} can transfer between resistance proteins that function in transport (MerT), sensing (MerR), and reduction (MerA) and foreshadowed the similar pathway described for the transfer of Cu^+ between chaperones and client proteins.[196,211] Similarly, the LMW thiols GSH and BSH are implicated in cytosolic trafficking of both zinc[167,184] and copper[197] and in assembly of FeS clusters.[147,212] Thiol-dependent ligand exchange reactions also underlie the ability of COG0523 family proteins to function as GTP-activated Zn^{2+} metallochaperones to direct the flow of Zn^{2+} to the most important client proteins under conditions of Zn limitation.[213−217] Like Hg^{2+}, copper trafficking often involves bis-coordination of Cu^+ ions by two thiolate groups with a transient addition of a third thiolate.[211] The resulting process of alternating 2- and 3-coordinate species provides an energetically accessible pathway for metal motion without ever releasing free (hydrated) Cu^+. This process provides a molecular basis for the function of copper storage proteins and metallochaperones in intracellular trafficking.[218]

CONCLUSION

Living systems rely on numerous inorganic ions that differ widely in their chemical behavior. Here, we have reviewed some of the key lessons that emerge from comparing the intracellular speciation of the major cellular cations. The labile cation pools are sensed by metalloregulatory systems[1,219] and serve to metalate nascent metalloproteins.[3] I have not included all biologically important metal ions, nor have I explored in detail the many interesting ways in which these labile pools compete for common ligands and how this can lead to mismetalation and toxicity.[3,158] In natural settings, microbes are often exposed to multimetal restriction[220] or to high concentrations of multiple metals,[221] which lead to complex combinatorial effects. Nor have I considered in detail the role of metallophores in accessing metals in the environment.[222] Nevertheless, the labile pools discussed here provide a framework for thinking about intracellular metal physiology.

This overview also reveals how far we still are from a detailed accounting of metal speciation and dynamics in even the best characterized model systems. Developing a more complete vision of microbial metal physiology will require a concerted effort by those conversant in disciplines ranging from

https://doi.org/10.1021/acs.biochem.4c00726
Biochemistry 2025, 64, 329−345

bioinorganic chemistry and structural biology to microbial genetics. Together with sensitive analytical tools, including an ever-increasing set of sensors to monitor chelatable metal ions in living cells,[223−225] it is becoming possible to better visualize metals in motion.

DEDICATION

My interest in metal physiology was motivated by experiences during my PhD studies at UC Berkeley and solidified during my time as a postdoctoral fellow with Chris Walsh. Although my graduate work with Mike Chamberlin was on bacterial RNA polymerase, the neighboring lab of Joe Neilands was exploring the role of siderophores in iron chelation,[226] and had just defined the role of Fur as an Fe^{2+}-dependent repressor of transcription.[227] Meanwhile, Imlay and Linn were exploring the role of labile iron pools in mediating the toxic consequences of hydrogen peroxide on bacterial viability.[228] Against this backdrop, and following a seminar visit by Chris Walsh, I read the seminal work from O'Halloran and Walsh defining the MerR protein as a Hg^{2+}-sensing transcription factor.[229] Intrigued by the notion of metalloregulation, I joined the Walsh group immediately following the lab's move from MIT to Harvard Medical School.

During my time as a postdoctoral fellow with Chris Walsh (1987−1990), I investigated the MerR metalloregulatory protein. Using a strategy involving site-directed mutagenesis and heterodimer complementation, I found that three Cys residues per protein dimer (C79 from one protomer, and C114 and C123 from the other) were necessary and sufficient for high affinity Hg^{2+} binding.[230] Experimentally, high affinity binding was defined using radioactive[203] Hg for detection and 10 mM β-mercaptoethanol as competitor. In later work, solution NMR studies revealed a planar, trigonal Hg^{2+} coordination.[231] Recent structural studies using X-ray crystallography support this geometry, but unexpectedly revealed a stoichiometry of two Hg^{2+} ions per protein dimer[232,233] rather than the single ion determined biochemically.[230,234] This likely resulted from the growth of crystals in the absence of LMW thiols or other metal buffers.

As others have recounted,[235,236] Chris Walsh was an inspirational mentor and a leader in chemical biology: the exploration of biological questions with the benefits and insights of chemical principles and intuition. My goal in the Walsh lab was to leverage my knowledge of bacterial RNA polymerase to understand the details of MerR-mediated regulation, an area where another former postdoctoral fellow, Tom O'Halloran, made major contributions.[237,238] This review is dedicated to Chris, and to all his mentees (formal and informal) who continue to build his legacy.

AUTHOR INFORMATION

Corresponding Author

John D. Helmann − *Department of Microbiology, Cornell University, Ithaca, New York 14853-8101, United States;* orcid.org/0000-0002-3832-3249; Email: jdh9@cornell.edu

Complete contact information is available at: https://pubs.acs.org/10.1021/acs.biochem.4c00726

Notes

The author declares no competing financial interest.

ACKNOWLEDGMENTS

I thank Arthur Glasfeld and the anonymous referees for their helpful comments. This work was supported by National Institutes of Health grant R35GM122461 awarded to JDH. The content is solely the responsibility of the authors and does not necessarily represent the official views of the National Institutes of Health.

ABBREVIATIONS

LMW, low molecular weight; BSH, bacillithiol; GSH, glutathione.

REFERENCES

(1) Chandrangsu, P.; Rensing, C.; Helmann, J. D. Metal homeostasis and resistance in bacteria. *Nat. Rev. Microbiol* **2017**, *15* (6), 338−350.

(2) Fraústo da Silva, J. J. R.; Williams, R. J. P. *The Biological Chemistry of the Elements: The Inorganic Chemistry of Life*; Oxford University Press, 2001.

(3) Foster, A. W.; Young, T. R.; Chivers, P. T.; Robinson, N. J. Protein metalation in biology. *Curr. Opin Chem. Biol.* **2022**, *66*, No. 102095.

(4) Osman, D.; Martini, M. A.; Foster, A. W.; Chen, J.; Scott, A. J. P.; Morton, R. J.; Steed, J. W.; Lurie-Luke, E.; Huggins, T. G.; Lawrence, A. D.; Deery, E.; Warren, M. J.; Chivers, P. T.; Robinson, N. J. Bacterial sensors define intracellular free energies for correct enzyme metalation. *Nat. Chem. Biol.* **2019**, *15* (3), 241−249.

(5) Nierhaus, K. H. Mg^{2+}, K^{+}, and the ribosome. *J. Bacteriol.* **2014**, *196* (22), 3817−3819.

(6) Sieg, J. P. A Divalent Metal Cation−Metabolite Interaction Model Reveals Cation Buffering and Speciation. *Biochemistry* **2024**, *63* (14), 1709−1717.

(7) Stautz, J.; Hellmich, Y.; Fuss, M. F.; Silberberg, J. M.; Devlin, J. R.; Stockbridge, R. B.; Hänelt, I. Molecular Mechanisms for Bacterial Potassium Homeostasis. *J. Mol. Biol.* **2021**, *433* (16), No. 166968.

(8) Papp-Wallace, K. M.; Maguire, M. E. Magnesium Transport and Magnesium Homeostasis. *EcoSal Plus* **2008**, DOI: 10.1128/ecosalplus.5.4.4.2.

(9) Danchin, A.; Nikel, P. I. Why Nature Chose Potassium. *J. Mol. Evol* **2019**, *87* (9−10), 271−288.

(10) Helmann, J. D. Specificity of metal sensing: iron and manganese homeostasis in Bacillus subtilis. *J. Biol. Chem.* **2014**, *289* (41), 28112−28120.

(11) Bosma, E. F.; Rau, M. H.; van Gijtenbeek, L. A.; Siedler, S. Regulation and distinct physiological roles of manganese in bacteria. *FEMS Microbiol. Rev.* **2021**, DOI: 10.1093/femsre/fuab028.

(12) Waldron, K. J.; Rutherford, J. C.; Ford, D.; Robinson, N. J. Metalloproteins and metal sensing. *Nature* **2009**, *460* (7257), 823−830.

(13) Arrhenius, S. ELECTROLYTIC DISSOCIATION. *J. Am. Chem. Soc.* **1912**, *34* (4), 353−364.

(14) Masa, J.; Barwe, S.; Andronescu, C.; Schuhmann, W. On the Theory of Electrolytic Dissociation, the Greenhouse Effect, and Activation Energy in (Electro)Catalysis: A Tribute to Svante Augustus Arrhenius. *Chem. Eur. J.* **2019**, *25* (1), 158−166.

(15) de Berg, K. C. The significance of the origin of physical chemistry for physical chemistry education: the case of electrolyte solution chemistry. *Chemistry Education Research and Practice* **2014**, *15* (3), 266−275.

(16) Crichton, R.; Pierre, J.-L. Old iron, young copper: from Mars to Venus. *Biometals* **2001**, *14*, 99−112.

(17) Johnson, J. E.; Present, T. M.; Valentine, J. S. Iron: Life's primeval transition metal. *Proc. Natl. Acad. Sci. U. S. A.* **2024**, *121* (38), No. e2318692121.

(18) LeBlanc, A. R.; Wuest, W. M. Siderophores: A Case Study in Translational Chemical Biology. *Biochemistry* **2024**, *63* (15), 1877−1891.

(19) Zhang, Y.; Sen, S.; Giedroc, D. P. Iron Acquisition by Bacterial Pathogens: Beyond Tris-Catecholate Complexes. *Chembiochem* **2020**, *21* (14), 1955−1967.
(20) Finney, L. A.; O'Halloran, T. V. Transition Metal Speciation in the Cell: Insights from the Chemistry of Metal Ion Receptors. *Science* **2003**, *300* (5621), 931−936.
(21) Irving, H.; Williams, R. J. P. Order of Stability of Metal Complexes. *Nature* **1948**, *162* (4123), 746−747.
(22) Hill, H. A. O.; Sadler, P. J. Bringing inorganic chemistry to life with inspiration from R. J. P. Williams. *JBIC Journal of Biological Inorganic Chemistry* **2016**, *21* (1), 5−12.
(23) Anderson, M. A.; Morel, F. M. M. The influence of aqueous iron chemistry on the uptake of iron by the coastal diatom *Thalassiosira weissflogii*. *Limnology and Oceanography* **1982**, *27* (5), 789−813.
(24) Outten, C. E.; O'Halloran, T. V. Femtomolar sensitivity of metalloregulatory proteins controlling zinc homeostasis. *Science* **2001**, *292* (5526), 2488−2492.
(25) Ma, Z.; Gabriel, S. E.; Helmann, J. D. Sequential binding and sensing of Zn(II) by *Bacillus subtilis* Zur. *Nucleic Acids Res.* **2011**, *39* (21), 9130−9138.
(26) Grossoehme, N. E.; Giedroc, D. P. Allosteric coupling between transition metal-binding sites in homooligomeric metal sensor proteins. *Methods Mol. Biol.* **2012**, *796*, 31−51.
(27) Kim, M.; Le, M. T.; Fan, L.; Campbell, C.; Sen, S.; Capdevila, D. A.; Stemmler, T. L.; Giedroc, D. P. Characterization of the Zinc Uptake Repressor (Zur) from *Acinetobacter baumannii*. *Biochemistry* **2024**, *63* (5), 660−670.
(28) Osman, D.; Foster, A. W.; Chen, J.; Svedaite, K.; Steed, J. W.; Lurie-Luke, E.; Huggins, T. G.; Robinson, N. J. Fine control of metal concentrations is necessary for cells to discern zinc from cobalt. *Nat. Commun.* **2017**, *8* (1), 1884.
(29) Dann, C. E., 3rd; Wakeman, C. A.; Sieling, C. L.; Baker, S. C.; Irnov, I.; Winkler, W. C. Structure and mechanism of a metal-sensing regulatory RNA. *Cell* **2007**, *130* (5), 878−892.
(30) Guerra, A. J.; Giedroc, D. P. Metal site occupancy and allosteric switching in bacterial metal sensor proteins. *Arch. Biochem. Biophys.* **2012**, *519* (2), 210−222.
(31) Stewart, L. J.; Thaqi, D.; Kobe, B.; McEwan, A. G.; Waldron, K. J.; Djoko, K. Y. Handling of nutrient copper in the bacterial envelope. *Metallomics* **2019**, *11* (1), 50−63.
(32) Krężel, A.; Maret, W. The biological inorganic chemistry of zinc ions. *Arch. Biochem. Biophys.* **2016**, *611*, 3−19.
(33) Goodsell, D. S. *Escherichia coli*. *Biochem Mol. Biol. Educ* **2009**, *37* (6), 325−332.
(34) Ellis, R. J.; Minton, A. P. Cell biology: join the crowd. *Nature* **2003**, *425* (6953), 27−28.
(35) Zimmerman, S. B.; Trach, S. O. Estimation of macromolecule concentrations and excluded volume effects for the cytoplasm of *Escherichia coli*. *J. Mol. Biol.* **1991**, *222* (3), 599−620.
(36) Record, M. T., Jr.; Courtenay, E. S.; Cayley, S.; Guttman, H. J. Biophysical compensation mechanisms buffering *E. coli* protein-nucleic acid interactions against changing environments. *Trends Biochem. Sci.* **1998**, *23* (5), 190−194.
(37) Cayley, S.; Lewis, B. A.; Guttman, H. J.; Record, M. T., Jr. Characterization of the cytoplasm of *Escherichia coli* K-12 as a function of external osmolarity. Implications for protein-DNA interactions in vivo. *J. Mol. Biol.* **1991**, *222* (2), 281−300.
(38) Parry, B. R.; Surovtsev, I. V.; Cabeen, M. T.; O'Hern, C. S.; Dufresne, E. R.; Jacobs-Wagner, C. The bacterial cytoplasm has glass-like properties and is fluidized by metabolic activity. *Cell* **2014**, *156* (1−2), 183−194.
(39) Kreuzer-Martin, H. W.; Ehleringer, J. R.; Hegg, E. L. Oxygen isotopes indicate most intracellular water in log-phase *Escherichia coli* is derived from metabolism. *Proc. Natl. Acad. Sci. U. S. A.* **2005**, *102* (48), 17337−17341.
(40) Ball, P. Water is an active matrix of life for cell and molecular biology. *Proc. Natl. Acad. Sci. U. S. A.* **2017**, *114* (51), 13327−13335.
(41) Record, M. T., Jr; Courtenay, E. S.; Cayley, D. S.; Guttman, H. J. Responses of *E. coli* to osmotic stress: large changes in amounts of cytoplasmic solutes and water. *Trends Biochem. Sci.* **1998**, *23* (4), 143−148.
(42) Brocchieri, L. Environmental signatures in proteome properties. *Proc. Natl. Acad. Sci. U. S. A.* **2004**, *101* (22), 8257−8258.
(43) Sieg, J. P.; McKinley, L. N.; Huot, M. J.; Yennawar, N. H.; Bevilacqua, P. C. The Metabolome Weakens RNA Thermodynamic Stability and Strengthens RNA Chemical Stability. *Biochemistry* **2022**, *61*, 2579.
(44) Remick, K. A.; Helmann, J. D. The elements of life: A biocentric tour of the periodic table. *Adv. Microb Physiol* **2023**, *82*, 1−127.
(45) Wood, J. M. Bacterial Osmoregulation: A Paradigm for the Study of Cellular Homeostasis. *Annu. Rev. Microbiol.* **2011**, *65*, 215−238.
(46) Foster, A. J.; van den Noort, M.; Poolman, B. Bacterial cell volume regulation and the importance of cyclic di-AMP. *Microbiol Mol. Biol. Rev.* **2024**, *88* (2), No. e0018123.
(47) Stülke, J.; Krüger, L. Cyclic di-AMP Signaling in Bacteria. *Annu. Rev. Microbiol.* **2020**, *74*, 159−179.
(48) Benarroch, J. M.; Asally, M. The microbiologist's guide to membrane potential dynamics. *Trends in microbiology* **2020**, *28* (4), 304−314.
(49) McLaggan, D.; Naprstek, J.; Buurman, E. T.; Epstein, W. Interdependence of K^+ and glutamate accumulation during osmotic adaptation of *Escherichia coli*. *J. Biol. Chem.* **1994**, *269* (3), 1911−1917.
(50) Roe, A. J.; McLaggan, D.; Davidson, I.; O'Byrne, C.; Booth, I. R. Perturbation of anion balance during inhibition of growth of *Escherichia coli* by weak acids. *J. Bacteriol.* **1998**, *180* (4), 767−772.
(51) Jenner, L. B.; Demeshkina, N.; Yusupova, G.; Yusupov, M. Structural aspects of messenger RNA reading frame maintenance by the ribosome. *Nat. Struct Mol. Biol.* **2010**, *17* (5), 555−560.
(52) Rozov, A.; Khusainov, I.; El Omari, K.; Duman, R.; Mykhaylyk, V.; Yusupov, M.; Westhof, E.; Wagner, A.; Yusupova, G. Importance of potassium ions for ribosome structure and function revealed by long-wavelength X-ray diffraction. *Nat. Commun.* **2019**, *10* (1), 2519.
(53) Tirumalai, M. R.; Rivas, M.; Tran, Q.; Fox, G. E. The Peptidyl Transferase Center: a Window to the Past. *Microbiol Mol. Biol. Rev.* **2021**, *85* (4), No. e0010421.
(54) Auffinger, P.; Ennifar, E.; D'Ascenzo, L. Deflating the RNA Mg(2+) bubble. Stereochemistry to the rescue! *RNA* **2021**, *27*, 243.
(55) Leonarski, F.; D'Ascenzo, L.; Auffinger, P. Nucleobase carbonyl groups are poor Mg(2+) inner-sphere binders but excellent monovalent ion binders-a critical PDB survey. *Rna* **2019**, *25* (2), 173−192.
(56) Bakshi, S.; Siryaporn, A.; Goulian, M.; Weisshaar, J. C. Superresolution imaging of ribosomes and RNA polymerase in live *Escherichia coli* cells. *Mol. Microbiol.* **2012**, *85* (1), 21−38.
(57) Gohara, D. W.; Di Cera, E. Molecular Mechanisms of Enzyme Activation by Monovalent Cations. *J. Biol. Chem.* **2016**, *291* (40), 20840−20848.
(58) Durdagi, S.; Roux, B.; Noskov, S. Y. Potassium-Binding Site Types in Proteins. In *Encyclopedia of Metalloproteins*; Kretsinger, R. H., Uversky, V. N., Permyakov, E. A., Eds.; Springer New York, 2013; pp 1809−1815.
(59) Toraya, T.; Sugimoto, Y.; Tamao, Y.; Shimizu, S.; Fukui, S. Propanediol dehydratase system. Role of monovalent cations in binding of vitamin B12 coenzyme or its analogs to apoenzyme. *Biochemistry* **1971**, *10* (18), 3475−3484.
(60) Pontes, M. H.; Sevostyanova, A.; Groisman, E. A. When Too Much ATP Is Bad for Protein Synthesis. *J. Mol. Biol.* **2015**, *427* (16), 2586−2594.
(61) Rauch, C.; Cherkaoui, M.; Egan, S.; Leigh, J. The bio-physics of condensation of divalent cations into the bacterial wall has implications for growth of Gram-positive bacteria. *Biochimica et Biophysica Acta (BBA)-Biomembranes* **2017**, *1859* (2), 282−288.
(62) Hoffmann, T. D.; Reeksting, B. J.; Gebhard, S. Bacteria-induced mineral precipitation: a mechanistic review. *Microbiology* **2021**, DOI: 10.1099/mic.0.001049.
(63) Lusk, J. E.; Williams, R. J.; Kennedy, E. P. Magnesium and the growth of *Escherichia coli*. *J. Biol. Chem.* **1968**, *243* (10), 2618−2624.

(64) Akanuma, G. Diverse relationships between metal ions and the ribosome. *Bioscience, biotechnology, and biochemistry* **2021**, *85* (7), 1582−1593.
(65) Zheng, H.; Shabalin, I. G.; Handing, K. B.; Bujnicki, J. M.; Minor, W. Magnesium-binding architectures in RNA crystal structures: validation, binding preferences, classification and motif detection. *Nucleic Acids Res.* **2015**, *43* (7), 3789−3801.
(66) Cowan, J. A. Understanding the Thermodynamics of Magnesium Binding to RNA Structural Motifs. *Life* **2024**, *14* (6), 765.
(67) Watson, Z. L.; Ward, F. R.; Méheust, R.; Ad, O.; Schepartz, A.; Banfield, J. F.; Cate, J. H. D. Structure of the bacterial ribosome at 2 Å resolution. *eLife* **2020**, *9*, No. e60482.
(68) Gucwa, M.; Lenkiewicz, J.; Zheng, H.; Cymborowski, M.; Cooper, D. R.; Murzyn, K.; Minor, W. CMM-An enhanced platform for interactive validation of metal binding sites. *Protein Sci.* **2023**, *32* (1), No. e4525.
(69) Moon, E. C.; Modi, T.; Lee, D. D.; Yangaliev, D.; Garcia-Ojalvo, J.; Ozkan, S. B.; Süel, G. M. Physiological cost of antibiotic resistance: Insights from a ribosome variant in bacteria. *Sci. Adv.* **2024**, *10* (46), No. eadq5249.
(70) Bray, M. S.; Lenz, T. K.; Haynes, J. W.; Bowman, J. C.; Petrov, A. S.; Reddi, A. R.; Hud, N. V.; Williams, L. D.; Glass, J. B. Multiple prebiotic metals mediate translation. *Proc. Natl. Acad. Sci. U. S. A.* **2018**, *115* (48), 12164−12169.
(71) Cowan, J. Structural and catalytic chemistry of magnesium-dependent enzymes. *Biometals* **2002**, *15*, 225−235.
(72) Froschauer, E. M.; Kolisek, M.; Dieterich, F.; Schweigel, M.; Schweyen, R. J. Fluorescence measurements of free [Mg^{2+}] by use of mag-fura 2 in *Salmonella enterica*. *FEMS Microbiol Lett.* **2004**, *237* (1), 49−55.
(73) Nemoto, T.; Tagashira, H.; Kita, T.; Kita, S.; Iwamoto, T. Functional characteristics and therapeutic potential of SLC41 transporters. *J. Pharmacol Sci.* **2023**, *151* (2), 88−92.
(74) Hattori, M.; Iwase, N.; Furuya, N.; Tanaka, Y.; Tsukazaki, T.; Ishitani, R.; Maguire, M. E.; Ito, K.; Maturana, A.; Nureki, O. Mg(2+)-dependent gating of bacterial MgtE channel underlies Mg(2+) homeostasis. *Embo j* **2009**, *28* (22), 3602−3612.
(75) Maruyama, T.; Imai, S.; Kusakizako, T.; Hattori, M.; Ishitani, R.; Nureki, O.; Ito, K.; Maturana, A. D.; Shimada, I.; Osawa, M. Functional roles of Mg(2+) binding sites in ion-dependent gating of a Mg(2+) channel, MgtE, revealed by solution NMR. *Elife* **2018**, DOI: 10.7554/eLife.31596.
(76) Kurz, J. C.; Fierke, C. A. The affinity of magnesium binding sites in the *Bacillus subtilis* RNase P x pre-tRNA complex is enhanced by the protein subunit. *Biochemistry* **2002**, *41* (30), 9545−9558.
(77) Wendel, B. M.; Pi, H.; Krüger, L.; Herzberg, C.; Stülke, J.; Helmann, J. D. A Central Role for Magnesium Homeostasis during Adaptation to Osmotic Stress. *mBio* **2022**, *13* (1), No. e0009222.
(78) Tang, R. J.; Meng, S. F.; Zheng, X. J.; Zhang, B.; Yang, Y.; Wang, C.; Fu, A. G.; Zhao, F. G.; Lan, W. Z.; Luan, S. Conserved mechanism for vacuolar magnesium sequestration in yeast and plant cells. *Nat. Plants* **2022**, *8* (2), 181−190.
(79) Raper, A. T.; Reed, A. J.; Suo, Z. Kinetic Mechanism of DNA Polymerases: Contributions of Conformational Dynamics and a Third Divalent Metal Ion. *Chem. Rev.* **2018**, *118* (12), 6000−6025.
(80) Gottesman, M. E.; Chudaev, M.; Mustaev, A. Key features of magnesium that underpin its role as the major ion for electrophilic biocatalysis. *Febs j* **2020**, *287* (24), 5439−5463.
(81) Meneely, K. M.; Sundlov, J. A.; Gulick, A. M.; Moran, G. R.; Lamb, A. L. An Open and Shut Case: The Interaction of Magnesium with MST Enzymes. *J. Am. Chem. Soc.* **2016**, *138* (29), 9277−9293.
(82) Sachla, A. J.; Soni, V.; Piñeros, M.; Luo, Y.; Im, J. J.; Rhee, K. Y.; Helmann, J. D. The *Bacillus subtilis yqgC-sodA* operon protects magnesium-dependent enzymes by supporting manganese efflux. *J. Bacteriol.* **2024**, *206*, No. e0005224.
(83) Pohland, A. C.; Schneider, D. Mg^{2+} homeostasis and transport in cyanobacteria - at the crossroads of bacterial and chloroplast Mg^{2+} import. *Biol. Chem.* **2019**, *400* (10), 1289−1301.
(84) Adams, N. B.; Brindley, A. A.; Hunter, C. N.; Reid, J. D. The catalytic power of magnesium chelatase: a benchmark for the AAA(+) ATPases. *FEBS Lett.* **2016**, *590* (12), 1687−1693.
(85) Tanaka, A.; Ito, H. Chlorophyll Degradation and its Physiological Function. *Plant Cell Physiol.* **2024**, DOI: 10.1093/pcp/pcae093.
(86) Peng, Y. Y.; Liao, L. L.; Liu, S.; Nie, M. M.; Li, J.; Zhang, L. D.; Ma, J. F.; Chen, Z. C. Magnesium Deficiency Triggers SGR-Mediated Chlorophyll Degradation for Magnesium Remobilization. *Plant Physiol* **2019**, *181* (1), 262−275.
(87) Dey, D.; Nishijima, M.; Tanaka, R.; Kurisu, G.; Tanaka, H.; Ito, H. Crystal structure and reaction mechanism of a bacterial Mg-dechelatase homolog from the Chloroflexi Anaerolineae. *Protein Sci.* **2022**, *31* (10), No. e4430.
(88) Sato, S.; Hirose, M.; Tanaka, R.; Ito, H.; Tamiaki, H. In vitro demetalation of central magnesium in various chlorophyll derivatives using Mg-dechelatase homolog from the chloroflexi Anaerolineae. *Photosynthesis Research* **2024**, *160* (1), 45−53.
(89) Anjem, A.; Varghese, S.; Imlay, J. A. Manganese import is a key element of the OxyR response to hydrogen peroxide in *Escherichia coli*. *Mol. Microbiol.* **2009**, *72* (4), 844−858.
(90) Faulkner, M. J.; Helmann, J. D. Peroxide stress elicits adaptive changes in bacterial metal ion homeostasis. *Antioxidants & redox signaling* **2011**, *15* (1), 175−189.
(91) Rohaun, S. K.; Sethu, R.; Imlay, J. A. Microbes vary strategically in their metalation of mononuclear enzymes. *Proc. Natl. Acad. Sci. U. S. A.* **2024**, *121* (21), No. e2401738121.
(92) Elli, M.; Zink, R.; Rytz, A.; Reniero, R.; Morelli, L. Iron requirement of *Lactobacillus* spp. in completely chemically defined growth media. *Journal of applied microbiology* **2000**, *88* (4), 695−703.
(93) Imbert, M.; Blondeau, R. On the iron requirement of lactobacilli grown in chemically defined medium. *Curr. Microbiol.* **1998**, *37* (1), 64−66.
(94) Posey, J. E.; Gherardini, F. C. Lack of a role for iron in the Lyme disease pathogen. *Science* **2000**, *288* (5471), 1651−1653.
(95) He, B.; Sachla, A. J.; Helmann, J. D. TerC proteins function during protein secretion to metalate exoenzymes. *Nat. Commun.* **2023**, *14* (1), 6186.
(96) He, B.; Helmann, J. D. Metalation of Extracytoplasmic Proteins and Bacterial Cell Envelope Homeostasis. *Annu. Rev. Microbiol.* **2024**, *78*, 83.
(97) Lisher, J. P.; Giedroc, D. P. Manganese acquisition and homeostasis at the host-pathogen interface. *Front Cell Infect Microbiol* **2013**, *3*, 91.
(98) Armstrong, F. A. Why did Nature choose manganese to make oxygen? *Philosophical Transactions of the Royal Society B: Biological Sciences* **2008**, *363* (1494), 1263−1270.
(99) Eisenhut, M. Manganese Homeostasis in Cyanobacteria. *Plants* **2020**, *9* (1), 18.
(100) Mrnjavac, N.; Degli Esposti, M.; Mizrahi, I.; Martin, W. F.; Allen, J. F. Three enzymes governed the rise of O_2 on Earth. *Biochimica et Biophysica Acta (BBA) - Bioenergetics* **2024**, *1865* (4), No. 149495.
(101) Ma, Z.; Faulkner, M. J.; Helmann, J. D. Origins of specificity and cross-talk in metal ion sensing by *Bacillus subtilis* Fur. *Mol. Microbiol.* **2012**, *86* (5), 1144−1155.
(102) Huang, X.; Shin, J. H.; Pinochet-Barros, A.; Su, T. T.; Helmann, J. D. *Bacillus subtilis* MntR coordinates the transcriptional regulation of manganese uptake and efflux systems. *Molecular microbiology* **2017**, *103* (2), 253−268.
(103) Price, I. R.; Gaballa, A.; Ding, F.; Helmann, J. D.; Ke, A. Mn^{2+}-Sensing Mechanisms of *yybP-ykoY* Orphan Riboswitches. *Mol. Cell* **2015**, *57* (6), 1110−1123.
(104) Tu, W. Y.; Pohl, S.; Gray, J.; Robinson, N. J.; Harwood, C. R.; Waldron, K. J. Cellular iron distribution in *Bacillus anthracis*. *J. Bacteriol.* **2012**, *194* (5), 932−940.
(105) Maass, S.; Sievers, S.; Zuhlke, D.; Kuzinski, J.; Sappa, P. K.; Muntel, J.; Hessling, B.; Bernhardt, J.; Sietmann, R.; Volker, U.; Hecker, M.; Becher, D. Efficient, global-scale quantification of absolute protein amounts by integration of targeted mass spectrometry and two-

dimensional gel-based proteomics. *Anal. Chem.* **2011**, *83* (7), 2677−2684.
(106) Tabares, L. C.; Un, S. In situ determination of manganese(II) speciation in Deinococcus radiodurans by high magnetic field EPR: detection of high levels of Mn(II) bound to proteins. *J. Biol. Chem.* **2013**, *288* (7), 5050−5055.
(107) Inaoka, T.; Matsumura, Y.; Tsuchido, T. SodA and manganese are essential for resistance to oxidative stress in growing and sporulating cells of *Bacillus subtilis*. *J. Bacteriol.* **1999**, *181* (6), 1939−1943.
(108) Turner, A. G.; Djoko, K. Y.; Ong, C. Y.; Barnett, T. C.; Walker, M. J.; McEwan, A. G. Group A Streptococcus co-ordinates manganese import and iron efflux in response to hydrogen peroxide stress. *Biochem. J.* **2019**, *476* (3), 595−611.
(109) Pinter, T. B.; Stillman, M. J. Kinetics of zinc and cadmium exchanges between metallothionein and carbonic anhydrase. *Biochemistry* **2015**, *54* (40), 6284−6293.
(110) Goodsell, D. S.; Dutta, S.; Zardecki, C.; Voigt, M.; Berman, H. M.; Burley, S. K. The RCSB PDB "Molecule of the Month": Inspiring a Molecular View of Biology. *PLOS Biology* **2015**, *13* (5), No. e1002140.
(111) Zardecki, C.; Dutta, S.; Goodsell, D. S.; Lowe, R.; Voigt, M.; Burley, S. K. PDB-101: Educational resources supporting molecular explorations through biology and medicine. *Protein Sci.* **2022**, *31* (1), 129−140.
(112) Murgas, C. J.; Green, S. P.; Forney, A. K.; Korba, R. M.; An, S. S.; Kitten, T.; Lucas, H. R. Intracellular Metal Speciation in *Streptococcus sanguinis* Establishes SsaACB as Critical for Redox Maintenance. *ACS Infect Dis* **2020**, *6* (7), 1906−1921.
(113) Bruch, E. M.; Thomine, S.; Tabares, L. C.; Un, S. Variations in Mn(II) speciation among organisms: what makes *D. radiodurans* different. *Metallomics* **2015**, *7* (1), 136−144.
(114) Daly, M. J.; Gaidamakova, E. K.; Matrosova, V. Y.; Vasilenko, A.; Zhai, M.; Venkateswaran, A.; Hess, M.; Omelchenko, M. V.; Kostandarithes, H. M.; Makarova, K. S.; Wackett, L. P.; Fredrickson, J. K.; Ghosal, D. Accumulation of Mn(II) in *Deinococcus radiodurans* facilitates gamma-radiation resistance. *Science* **2004**, *306* (5698), 1025−1028.
(115) Culotta, V. C.; Daly, M. J. Manganese complexes: diverse metabolic routes to oxidative stress resistance in prokaryotes and yeast. *Antioxid Redox Signal* **2013**, *19* (9), 933−944.
(116) Slade, D.; Radman, M. Oxidative stress resistance in *Deinococcus radiodurans*. *Microbiol Mol. Biol. Rev.* **2011**, *75* (1), 133−191.
(117) McNaughton, R. L.; Reddi, A. R.; Clement, M. H.; Sharma, A.; Barnese, K.; Rosenfeld, L.; Gralla, E. B.; Valentine, J. S.; Culotta, V. C.; Hoffman, B. M. Probing in vivo Mn^{2+} speciation and oxidative stress resistance in yeast cells with electron-nuclear double resonance spectroscopy. *Proc. Natl. Acad. Sci. U. S. A.* **2010**, *107* (35), 15335−15339.
(118) Merchant, S. S.; Helmann, J. D. Elemental economy: microbial strategies for optimizing growth in the face of nutrient limitation. *Adv. Microb Physiol* **2012**, *60*, 91−210.
(119) Cassat, J. E.; Skaar, E. P. Iron in infection and immunity. *Cell Host Microbe* **2013**, *13* (5), 509−519.
(120) Murdoch, C. C.; Skaar, E. P. Nutritional immunity: the battle for nutrient metals at the host−pathogen interface. *Nature Reviews Microbiology* **2022**, *20* (11), 657−670.
(121) Gerner, R. R.; Nuccio, S.-P.; Raffatellu, M. Iron at the host-microbe interface. *Molecular Aspects of Medicine* **2020**, *75*, No. 100895.
(122) Faulkner, M. J.; Ma, Z.; Fuangthong, M.; Helmann, J. D. Derepression of the *Bacillus subtilis* PerR peroxide stress response leads to iron deficiency. *J. Bacteriol.* **2012**, *194* (5), 1226−1235.
(123) Keyer, K.; Imlay, J. A. Superoxide accelerates DNA damage by elevating free-iron levels. *Proc. Natl. Acad. Sci. U. S. A.* **1996**, *93* (24), 13635−13640.
(124) Brawley, H. N.; Kreinbrink, A. C.; Hierholzer, J. D.; Vali, S. W.; Lindahl, P. A. Labile Iron Pool of Isolated *Escherichia coli* Cytosol Likely Includes Fe-ATP and Fe-Citrate but not Fe-Glutathione or Aqueous Fe. *J. Am. Chem. Soc.* **2023**, *145* (4), 2104−2117.
(125) Bradley, J. M.; Svistunenko, D. A.; Wilson, M. T.; Hemmings, A. M.; Moore, G. R.; Le Brun, N. E. Bacterial iron detoxification at the molecular level. *J. Biol. Chem.* **2020**, *295* (51), 17602−17623.
(126) Arosio, P.; Elia, L.; Poli, M. Ferritin, cellular iron storage and regulation. *IUBMB Life* **2017**, *69* (6), 414−422.
(127) Honarmand Ebrahimi, K.; Hagedoorn, P.-L.; Hagen, W. R. Unity in the Biochemistry of the Iron-Storage Proteins Ferritin and Bacterioferritin. *Chem. Rev.* **2015**, *115* (1), 295−326.
(128) Williams, S. M.; Chatterji, D. Dps Functions as a Key Player in Bacterial Iron Homeostasis. *ACS Omega* **2023**, *8* (38), 34299−34309.
(129) Rivera, M. Bacterioferritin: Structure, Dynamics, and Protein−Protein Interactions at Play in Iron Storage and Mobilization. *Acc. Chem. Res.* **2017**, *50* (2), 331−340.
(130) Abdul-Tehrani, H.; Hudson, A. J.; Chang, Y. S.; Timms, A. R.; Hawkins, C.; Williams, J. M.; Harrison, P. M.; Guest, J. R.; Andrews, S. C. Ferritin mutants of *Escherichia coli* are iron deficient and growth impaired, and fur mutants are iron deficient. *J. Bacteriol.* **1999**, *181* (5), 1415−1428.
(131) Andrews, S. C. Iron storage in bacteria. *Adv. Microb Physiol* **1998**, *40*, 281−351.
(132) Smith, G. L.; Srivastava, A. K.; Reutovich, A. A.; Hunter, N. J.; Arosio, P.; Melman, A.; Bou-Abdallah, F. Iron Mobilization from Ferritin in Yeast Cell Lysate and Physiological Implications. *Int. J. Mol. Sci.* **2022**, *23* (11), 6100.
(133) Sen, A.; Zhou, Y.; Imlay, J. A. During Oxidative Stress the Clp Proteins of *Escherichia coli* Ensure that Iron Pools Remain Sufficient To Reactivate Oxidized Metalloenzymes. *J. Bacteriol.* **2020**, DOI: 10.1128/JB.00235-20.
(134) Pi, H.; Sun, R.; McBride, J. R.; Kruse, A. R. S.; Gibson-Corley, K. N.; Krystofiak, E. S.; Nicholson, M. R.; Spraggins, J. M.; Zhou, Q.; Skaar, E. P. *Clostridioides difficile* ferrosome organelles combat nutritional immunity. *Nature* **2023**, *623* (7989), 1009−1016.
(135) Grant, C. R.; Amor, M.; Trujillo, H. A.; Krishnapura, S.; Iavarone, A. T.; Komeili, A. Distinct gene clusters drive formation of ferrosome organelles in bacteria. *Nature* **2022**, *606* (7912), 160−164.
(136) Brown, J. B.; Lee, M. A.; Smith, A. T. Ins and Outs: Recent Advancements in Membrane Protein-Mediated Prokaryotic Ferrous Iron Transport. *Biochemistry* **2021**, *60* (44), 3277−3291.
(137) Pi, H.; Helmann, J. D. Ferrous iron efflux systems in bacteria. *Metallomics* **2017**, *9* (7), 840−851.
(138) Guan, G.; Pinochet-Barros, A.; Gaballa, A.; Patel, S. J.; Argüello, J. M.; Helmann, J. D. PfeT, a P_{1B4} -type ATPase, effluxes ferrous iron and protects *Bacillus subtilis* against iron intoxication. *Mol. Microbiol.* **2015**, *98* (4), 787−803.
(139) Pi, H.; Patel, S. J.; Argüello, J. M.; Helmann, J. D. The *Listeria monocytogenes* Fur-regulated virulence protein FrvA is an Fe(II) efflux P_{1B4} -type ATPase. *Mol. Microbiol.* **2016**, *100* (6), 1066−1079.
(140) Pinochet-Barros, A.; Helmann, J. D. *Bacillus subtilis* Fur Is a Transcriptional Activator for the PerR-Repressed *pfeT* Gene, Encoding an Iron Efflux Pump. *J. Bacteriol.* **2020**, DOI: 10.1128/JB.00697-19.
(141) Mills, S. A.; Marletta, M. A. Metal binding characteristics and role of iron oxidation in the ferric uptake regulator from *Escherichia coli*. *Biochemistry* **2005**, *44* (41), 13553−13559.
(142) Brawley, H. N.; Lindahl, P. A. Low-molecular-mass labile metal pools in *Escherichia coli*: advances using chromatography and mass spectrometry. *J. Biol. Inorg. Chem.* **2021**, *26* (4), 479−494.
(143) Hider, R. C.; Kong, X. L. Glutathione: a key component of the cytoplasmic labile iron pool. *Biometals* **2011**, *24* (6), 1179−1187.
(144) Philpott, C. C.; Patel, S. J.; Protchenko, O. Management versus miscues in the cytosolic labile iron pool: The varied functions of iron chaperones. *Biochim Biophys Acta Mol. Cell Res.* **2020**, *1867* (11), No. 118830.
(145) Chandrangsu, P.; Loi, V. V.; Antelmann, H.; Helmann, J. D. The Role of Bacillithiol in Gram-Positive Firmicutes. *Antioxid Redox Signal* **2018**, *28* (6), 445−462.
(146) Fang, Z.; Dos Santos, P. C. Protective role of bacillithiol in superoxide stress and Fe-S metabolism in *Bacillus subtilis*. *Microbiologyopen* **2015**, *4* (4), 616−631.

(147) Rosario-Cruz, Z.; Chahal, H. K.; Mike, L. A.; Skaar, E. P.; Boyd, J. M. Bacillithiol has a role in Fe-S cluster biogenesis in *Staphylococcus aureus*. *Mol. Microbiol.* **2015**, *98* (2), 218−242.
(148) Williams, R. J. Free manganese (II) and iron (II) cations can act as intracellular cell controls. *FEBS Lett.* **1982**, *140* (1), 3−10.
(149) Kandari, D.; Joshi, H. PerR: A Peroxide Sensor Eliciting Metal Ion-dependent Regulation in Various Bacteria. *Mol. Biotechnol* **2024**, DOI: 10.1007/s12033-024-01266-8.
(150) Lee, J. W.; Helmann, J. D. The PerR transcription factor senses H_2O_2 by metal-catalysed histidine oxidation. *Nature* **2006**, *440* (7082), 363−367.
(151) Helmann, J. D.; Wu, M. F.; Gaballa, A.; Kobel, P. A.; Morshedi, M. M.; Fawcett, P.; Paddon, C. The global transcriptional response of *Bacillus subtilis* to peroxide stress is coordinated by three transcription factors. *J. Bacteriol.* **2003**, *185* (1), 243−253.
(152) Mostertz, J.; Scharf, C.; Hecker, M.; Homuth, G. Transcriptome and proteome analysis of *Bacillus subtilis* gene expression in response to superoxide and peroxide stress. *Microbiology* **2004**, *150* (2), 497−512.
(153) Fuangthong, M.; Herbig, A. F.; Bsat, N.; Helmann, J. D. Regulation of the *Bacillus subtilis fur* and *perR* genes by PerR: not all members of the PerR regulon are peroxide inducible. *J. Bacteriol.* **2002**, *184* (12), 3276−3286.
(154) Chandrangsu, P.; Helmann, J. D. Intracellular Zn(II) Intoxication Leads to Dysregulation of the PerR Regulon Resulting in Heme Toxicity in *Bacillus subtilis*. *PLoS Genet* **2016**, *12* (12), No. e1006515.
(155) Wakeman, C. A.; Hammer, N. D.; Stauff, D. L.; Attia, A. S.; Anzaldi, L. L.; Dikalov, S. I.; Calcutt, M. W.; Skaar, E. P. Menaquinone biosynthesis potentiates haem toxicity in *Staphylococcus aureus*. *Mol. Microbiol.* **2012**, *86* (6), 1376−1392.
(156) Choby, J. E.; Skaar, E. P. Heme Synthesis and Acquisition in Bacterial Pathogens. *J. Mol. Biol.* **2016**, *428* (17), 3408−3428.
(157) Imlay, J. A. The molecular mechanisms and physiological consequences of oxidative stress: lessons from a model bacterium. *Nature Reviews Microbiology* **2013**, *11* (7), 443−454.
(158) Barwinska-Sendra, A.; Waldron, K. J. The role of intermetal competition and mis-metalation in metal toxicity. *Advances in Microbial Physiology* **2017**, *70*, 315−379.
(159) Chareyre, S.; Mandin, P. Bacterial Iron Homeostasis Regulation by sRNAs. *Microbiol. Spectrum* **2018**, DOI: 10.1128/microbiolspec.RWR-0010-2017.
(160) Oglesby-Sherrouse, A. G.; Murphy, E. R. Iron-responsive bacterial small RNAs: variations on a theme. *Metallomics* **2013**, *5* (4), 276−286.
(161) Gaballa, A.; Antelmann, H.; Aguilar, C.; Khakh, S. K.; Song, K.-B.; Smaldone, G. T.; Helmann, J. D. The *Bacillus subtilis* iron-sparing response is mediated by a Fur-regulated small RNA and three small, basic proteins. *Proc. Natl. Acad. Sci. U. S. A.* **2008**, *105* (33), 11927−11932.
(162) Saito, M. A.; Bertrand, E. M.; Dutkiewicz, S.; Bulygin, V. V.; Moran, D. M.; Monteiro, F. M.; Follows, M. J.; Valois, F. W.; Waterbury, J. B. Iron conservation by reduction of metalloenzyme inventories in the marine diazotroph *Crocosphaera watsonii*. *Proc. Natl. Acad. Sci. U. S. A.* **2011**, *108* (6), 2184−2189.
(163) Dudev, T.; Lim, C. Competition among metal ions for protein binding sites: determinants of metal ion selectivity in proteins. *Chem. Rev.* **2014**, *114* (1), 538−556.
(164) Wang, D.; Fierke, C. A. The BaeSR regulon is involved in defense against zinc toxicity in *E. coli*. *Metallomics* **2013**, *5* (4), 372−383.
(165) Mikhaylina, A.; Ksibe, A. Z.; Wilkinson, R. C.; Smith, D.; Marks, E.; Coverdale, J. P. C.; Fülöp, V.; Scanlan, D. J.; Blindauer, C. A. A single sensor controls large variations in zinc quotas in a marine cyanobacterium. *Nat. Chem. Biol.* **2022**, *18* (8), 869−877.
(166) Herzberg, M.; Dobritzsch, D.; Helm, S.; Baginsky, S.; Nies, D. H. The zinc repository of *Cupriavidus metallidurans*. *Metallomics* **2014**, *6* (11), 2157−2165.
(167) Ma, Z.; Chandrangsu, P.; Helmann, T. C.; Romsang, A.; Gaballa, A.; Helmann, J. D. Bacillithiol is a major buffer of the labile zinc pool in *Bacillus subtilis*. *Molecular microbiology* **2014**, *94* (4), 756−770.
(168) Imlay, J. A. The mismetallation of enzymes during oxidative stress. *J. Biol. Chem.* **2014**, *289* (41), 28121−28128.
(169) Wang, Y.; Weisenhorn, E.; MacDiarmid, C. W.; Andreini, C.; Bucci, M.; Taggart, J.; Banci, L.; Russell, J.; Coon, J. J.; Eide, D. J. The cellular economy of the *Saccharomyces cerevisiae* zinc proteome. *Metallomics* **2018**, *10* (12), 1755−1776.
(170) Maret, W.; Li, Y. Coordination Dynamics of Zinc in Proteins. *Chem. Rev.* **2009**, *109* (10), 4682−4707.
(171) Chong, C. R.; Auld, D. S. Catalysis of zinc transfer by D-penicillamine to secondary chelators. *J. Med. Chem.* **2007**, *50* (22), 5524−5527.
(172) Sobota, J. M.; Imlay, J. A. Iron enzyme ribulose-5-phosphate 3-epimerase in *Escherichia coli* is rapidly damaged by hydrogen peroxide but can be protected by manganese. *Proc. Natl. Acad. Sci. U. S. A.* **2011**, *108* (13), 5402−5407.
(173) Gu, M.; Imlay, J. A. Superoxide poisons mononuclear iron enzymes by causing mismetallation. *Mol. Microbiol.* **2013**, *89* (1), 123−134.
(174) Nanamiya, H.; Akanuma, G.; Natori, Y.; Murayama, R.; Kosono, S.; Kudo, T.; Kobayashi, K.; Ogasawara, N.; Park, S.-M.; Ochi, K.; Kawamura, F. Zinc is a key factor in controlling alternation of two types of L31 protein in the *Bacillus subtilis* ribosome. *Mol. Microbiol.* **2004**, *52* (1), 273−283.
(175) Gabriel, S. E.; Helmann, J. D. Contributions of Zur-controlled ribosomal proteins to growth under zinc starvation conditions. *Journal of bacteriology* **2009**, *191* (19), 6116−6122.
(176) Hensley, M. P.; Tierney, D. L.; Crowder, M. W. Zn(II) binding to *Escherichia coli* 70S ribosomes. *Biochemistry* **2011**, *50* (46), 9937−9939.
(177) Shin, J. H.; Helmann, J. D. Molecular logic of the Zur-regulated zinc deprivation response in *Bacillus subtilis*. *Nat. Commun.* **2016**, *7*, No. 12612.
(178) Colvin, R. A.; Holmes, W. R.; Fontaine, C. P.; Maret, W. Cytosolic zinc buffering and muffling: their role in intracellular zinc homeostasis. *Metallomics* **2010**, *2* (5), 306−317.
(179) Helbig, K.; Bleuel, C.; Krauss, G. J.; Nies, D. H. Glutathione and transition-metal homeostasis in *Escherichia coli*. *J. Bacteriol.* **2008**, *190* (15), 5431−5438.
(180) Shin, J.-H.; Jung, H. J.; An, Y. J.; Cho, Y.-B.; Cha, S.-S.; Roe, J.-H. Graded expression of zinc-responsive genes through two regulatory zinc-binding sites in Zur. *Proc. Natl. Acad. Sci. U. S. A.* **2011**, *108* (12), 5045−5050.
(181) Kochańczyk, T.; Drozd, A.; Krężel, A. Relationship between the architecture of zinc coordination and zinc binding affinity in proteins–insights into zinc regulation. *Metallomics* **2015**, *7* (2), 244−257.
(182) Helmann, J. D. Bacillithiol, a new player in bacterial redox homeostasis. *Antioxid Redox Signal* **2011**, *15* (1), 123−133.
(183) Sharma, S. V.; Arbach, M.; Roberts, A. A.; Macdonald, C. J.; Groom, M.; Hamilton, C. J. Biophysical features of bacillithiol, the glutathione surrogate of *Bacillus subtilis* and other firmicutes. *Chembiochem* **2013**, *14* (16), 2160−2168.
(184) Rosario-Cruz, Z.; Boyd, J. M. Physiological roles of bacillithiol in intracellular metal processing. *Curr. Genet* **2016**, *62* (1), 59−65.
(185) Pratt, E. P. S.; Damon, L. J.; Anson, K. J.; Palmer, A. E. Tools and techniques for illuminating the cell biology of zinc. *Biochim Biophys Acta Mol. Cell Res.* **2021**, *1868* (1), No. 118865.
(186) Maret, W. Analyzing free zinc(II) ion concentrations in cell biology with fluorescent chelating molecules. *Metallomics* **2015**, *7* (2), 202−211.
(187) Antoine, R.; Rivera-Millot, A.; Roy, G.; Jacob-Dubuisson, F. Relationships between copper-related proteomes and lifestyles in β proteobacteria. *Front. Microbiol.* **2019**, *10*, 2217.
(188) Zhang, Y.; Zheng, J. Bioinformatics of Metalloproteins and Metalloproteomes. *Molecules* **2020**, *25* (15), 3366.
(189) Changela, A.; Chen, K.; Xue, Y.; Holschen, J.; Outten, C. E.; O'Halloran, T. V.; Mondragón, A. Molecular Basis of Metal-Ion

Selectivity and Zeptomolar Sensitivity by CueR. *Science* **2003**, *301* (5638), 1383−1387.
(190) Galea, D.; Herzberg, M.; Nies, D. H. The metal-binding GTPases CobW2 and CobW3 are at the crossroads of zinc and cobalt homeostasis in *Cupriavidus metallidurans*. *J. Bacteriol.* **2024**, *206*, e00226-24.
(191) Chillappagari, S.; Miethke, M.; Trip, H.; Kuipers, O. P.; Marahiel, M. A. Copper Acquisition Is Mediated by YcnJ and Regulated by YcnK and CsoR in *Bacillus subtilis*. *J. Bacteriol.* **2009**, *191* (7), 2362−2370.
(192) Merchant, S. S.; Schmollinger, S.; Strenkert, D.; Moseley, J. L.; Blaby-Haas, C. E. From economy to luxury: Copper homeostasis in *Chlamydomonas* and other algae. *Biochimica et Biophysica Acta (BBA) - Molecular Cell Research* **2020**, *1867* (11), No. 118822.
(193) Rensing, C.; McDevitt, S. F. The Copper Metallome in Prokaryotic Cells. In *Metallomics and the Cell*; Banci, L., Ed.; Springer Netherlands, 2013; pp 417−450.
(194) Han, J. Copper trafficking systems in cells: insights into coordination chemistry and toxicity. *Dalton Trans* **2023**, *52* (42), 15277−15296.
(195) Robinson, N. J.; Winge, D. R. Copper metallochaperones. *Annu. Rev. Biochem.* **2010**, *79*, 537−562.
(196) Andrei, A.; Öztürk, Y.; Khalfaoui-Hassani, B.; Rauch, J.; Marckmann, D.; Trasnea, P.-I.; Daldal, F.; Koch, H.-G. Cu Homeostasis in Bacteria: The Ins and Outs. *Membranes* **2020**, *10* (9), 242.
(197) Stewart, L. J.; Ong, C. Y.; Zhang, M. M.; Brouwer, S.; McIntyre, L.; Davies, M. R.; Walker, M. J.; McEwan, A. G.; Waldron, K. J.; Djoko, K. Y. Role of Glutathione in Buffering Excess Intracellular Copper in *Streptococcus pyogenes*. *mBio* **2020**, DOI: 10.1128/mBio.02804-20.
(198) Kay, K. L.; Hamilton, C. J.; Le Brun, N. E. Mass spectrometric studies of Cu(I)-binding to the N-terminal domains of *B. subtilis* CopA and influence of bacillithiol. *J. Inorg. Biochem* **2019**, *190*, 24−30.
(199) Strenkert, D.; Schmollinger, S.; Hu, Y.; Hofmann, C.; Holbrook, K.; Liu, H. W.; Purvine, S. O.; Nicora, C. D.; Chen, S.; Lipton, M. S.; Northen, T. R.; Clemens, S.; Merchant, S. S. Zn deficiency disrupts Cu and S homeostasis in *Chlamydomonas* resulting in over accumulation of Cu and Cysteine. *Metallomics* **2023**, DOI: 10.1093/mtomcs/mfad043.
(200) Morgan, M. T.; Bourassa, D.; Harankhedkar, S.; McCallum, A. M.; Zlatic, S. A.; Calvo, J. S.; Meloni, G.; Faundez, V.; Fahrni, C. J. Ratiometric two-photon microscopy reveals attomolar copper buffering in normal and Menkes mutant cells. *Proc. Natl. Acad. Sci. U. S. A.* **2019**, *116* (25), 12167−12172.
(201) Rae, T. D.; Schmidt, P. J.; Pufahl, R. A.; Culotta, V. C.; O'Halloran, T. V. Undetectable intracellular free copper: the requirement of a copper chaperone for superoxide dismutase. *Science* **1999**, *284* (5415), 805−808.
(202) Calvo, J.; Jung, H.; Meloni, G. Copper metallothioneins. *IUBMB Life* **2017**, *69* (4), 236−245.
(203) Gold, B.; Deng, H.; Bryk, R.; Vargas, D.; Eliezer, D.; Roberts, J.; Jiang, X.; Nathan, C. Identification of a copper-binding metallothionein in pathogenic mycobacteria. *Nat. Chem. Biol.* **2008**, *4* (10), 609−616.
(204) Dennison, C.; David, S.; Lee, J. Bacterial copper storage proteins. *J. Biol. Chem.* **2018**, *293* (13), 4616−4627.
(205) Vita, N.; Landolfi, G.; Baslé, A.; Platsaki, S.; Lee, J.; Waldron, K. J.; Dennison, C. Bacterial cytosolic proteins with a high capacity for Cu(I) that protect against copper toxicity. *Sci. Rep.* **2016**, *6* (1), No. 39065.
(206) Dennison, C. The Coordination Chemistry of Copper Uptake and Storage for Methane Oxidation. *Chemistry* **2019**, *25* (1), 74−86.
(207) Vita, N.; Platsaki, S.; Baslé, A.; Allen, S. J.; Paterson, N. G.; Crombie, A. T.; Murrell, J. C.; Waldron, K. J.; Dennison, C. A four-helix bundle stores copper for methane oxidation. *Nature* **2015**, *525* (7567), 140−143.
(208) Lee, J.; Dalton, R. A.; Dennison, C. Copper delivery to an endospore coat protein of Bacillus subtilis. *Front Cell Dev Biol.* **2022**, *10*, No. 916114.
(209) Barkay, T.; Miller, S. M.; Summers, A. O. Bacterial mercury resistance from atoms to ecosystems. *FEMS Microbiol Rev.* **2003**, *27* (2−3), 355−384.
(210) Cheesman, B. V.; Arnold, A. P.; Rabenstein, D. L. Nuclear magnetic resonance studies of the solution chemistry of metal complexes. 25. Hg (thiol) 3 complexes and Hg (II)-thiol ligand exchange kinetics. *J. Am. Chem. Soc.* **1988**, *110* (19), 6359−6364.
(211) Rosenzweig, A. C. Copper delivery by metallochaperone proteins. *Acc. Chem. Res.* **2001**, *34* (2), 119−128.
(212) Fidai, I.; Wachnowsky, C.; Cowan, J. A. Glutathione-complexed [2Fe-2S] clusters function in Fe-S cluster storage and trafficking. *J. Biol. Inorg. Chem.* **2016**, *21* (7), 887−901.
(213) Haas, C. E.; Rodionov, D. A.; Kropat, J.; Malasarn, D.; Merchant, S. S.; de Crécy-Lagard, V. A subset of the diverse COG0523 family of putative metal chaperones is linked to zinc homeostasis in all kingdoms of life. *BMC Genomics* **2009**, *10*, 470.
(214) Chandrangsu, P.; Huang, X.; Gaballa, A.; Helmann, J. D. *Bacillus subtilis* FolE is sustained by the ZagA zinc metallochaperone and the alarmone ZTP under conditions of zinc deficiency. *Mol. Microbiol.* **2019**, *112* (3), 751−765.
(215) Edmonds, K. A.; Jordan, M. R.; Giedroc, D. P. COG0523 proteins: a functionally diverse family of transition metal-regulated G3E P-loop GTP hydrolases from bacteria to man. *Metallomics* **2021**, DOI: 10.1093/mtomcs/mfab046.
(216) Pasquini, M.; Grosjean, N.; Hixson, K. K.; Nicora, C. D.; Yee, E. F.; Lipton, M.; Blaby, I. K.; Haley, J. D.; Blaby-Haas, C. E. Zng1 is a GTP-dependent zinc transferase needed for activation of methionine aminopeptidase. *Cell Rep* **2022**, *39* (7), No. 110834.
(217) Weiss, A.; Murdoch, C. C.; Edmonds, K. A.; Jordan, M. R.; Monteith, A. J.; Perera, Y. R.; Rodríguez Nassif, A. M.; Petoletti, A. M.; Beavers, W. N.; Munneke, M. J.; Drury, S. L.; Krystofiak, E. S.; Thalluri, K.; Wu, H.; Kruse, A. S.; DiMarchi, R. D.; Caprioli, R. M.; Spraggins, J. M.; Chazin, W. J.; Giedroc, D. P.; Skaar, E. P. Zn-regulated GTPase metalloprotein activator 1 modulates vertebrate zinc homeostasis. *Cell* **2022**, *185* (12), 2148−2163.
(218) O'Halloran, T. V.; Culotta, V. C. Metallochaperones, an intracellular shuttle service for metal ions. *J. Biol. Chem.* **2000**, *275* (33), 25057−25060.
(219) Capdevila, D. A.; Edmonds, K. A.; Giedroc, D. P. Metallochaperones and metalloregulation in bacteria. *Essays Biochem.* **2017**, *61* (2), 177−200.
(220) Jordan, M. R.; Wang, J.; Capdevila, D. A.; Giedroc, D. P. Multi-metal nutrient restriction and crosstalk in metallostasis systems in microbial pathogens. *Curr. Opin Microbiol* **2020**, *55*, 17−25.
(221) Goff, J. L.; Chen, Y.; Thorgersen, M. P.; Hoang, L. T.; Poole, F. L., 2nd; Szink, E. G.; Siuzdak, G.; Petzold, C. J.; Adams, M. W. W. Mixed heavy metal stress induces global iron starvation response. *Isme j* **2023**, *17* (3), 382−392.
(222) Maret, W. The Extracellular Metallometabolome: Metallophores, Metal Ionophores, and Other Chelating Agents as Natural Products. *Nat. Prod. Commun.* **2024**, *19* (8), No. 1934578X241271701, DOI: 10.1177/1934578X241271701.
(223) Jensen, G. C.; Janis, M. K.; Nguyen, H. N.; David, O. W.; Zastrow, M. L. Fluorescent Protein-Based Sensors for Detecting Essential Metal Ions across the Tree of Life. *ACS Sens.* **2024**, *9* (4), 1622−1643.
(224) Grover, K.; Koblova, A.; Pezacki, A. T.; Chang, C. J.; New, E. J. Small-Molecule Fluorescent Probes for Binding- and Activity-Based Sensing of Redox-Active Biological Metals. *Chem. Rev.* **2024**, *124* (9), 5846−5929.
(225) Torres-Ocampo, A. P.; Palmer, A. E. Genetically encoded fluorescent sensors for metals in biology. *Curr. Opin Chem. Biol.* **2023**, *74*, No. 102284.
(226) Neilands, J. B. Siderophores: structure and function of microbial iron transport compounds. *J. Biol. Chem.* **1995**, *270* (45), 26723−26726.
(227) Bagg, A.; Neilands, J. B. Ferric uptake regulation protein acts as a repressor, employing iron (II) as a cofactor to bind the operator of an iron transport operon in *Escherichia coli*. *Biochemistry* **1987**, *26* (17), 5471−5477.
(228) Imlay, J. A.; Linn, S. DNA damage and oxygen radical toxicity. *Science* **1988**, *240* (4857), 1302−1309.

(229) O'Halloran, T.; Walsh, C. Metalloregulatory DNA-binding protein encoded by the *merR* gene: isolation and characterization. *Science* **1987**, *235* (4785), 211−214.
(230) Helmann, J. D.; Ballard, B. T.; Walsh, C. T. The MerR metalloregulatory protein binds mercuric ion as a tricoordinate, metal-bridged dimer. *Science* **1990**, *247* (4945), 946−948.
(231) Utschig, L. M.; Bryson, J. W.; O'Halloran, T. V. Mercury-199 NMR of the metal receptor site in MerR and its protein-DNA complex. *Science* **1995**, *268* (5209), 380−385.
(232) Chang, C.-C.; Lin, L.-Y.; Zou, X.-W.; Huang, C.-C.; Chan, N.-L. Structural basis of the mercury(II)-mediated conformational switching of the dual-function transcriptional regulator MerR. *Nucleic Acids Res.* **2015**, *43* (15), 7612−7623.
(233) Wang, D.; Huang, S.; Liu, P.; Liu, X.; He, Y.; Chen, W.; Hu, Q.; Wei, T.; Gan, J.; Ma, J.; Chen, H. Structural Analysis of the Hg(II)-Regulatory Protein Tn501 MerR from *Pseudomonas aeruginosa*. *Sci. Rep* **2016**, *6*, No. 33391.
(234) Shewchuk, L. M.; Verdine, G. L.; Walsh, C. T. Transcriptional switching by the metalloregulatory MerR protein: initial characterization of DNA and mercury (II) binding activities. *Biochemistry* **1989**, *28* (5), 2331−2339.
(235) O'Halloran, T. V. Christopher T. Walsh (1944−2023). *Science* **2023**, *379* (6634), 762−762.
(236) Lin, H. Christopher T. Walsh: A Prolific Scientist, Effective Academic Leader, and Responsive Mentor. *ACS Chem. Biol.* **2023**, *18* (4), 668−670.
(237) O'Halloran, T. V.; Frantz, B.; Shin, M. K.; Ralston, D. M.; Wright, J. G. The MerR heavy metal receptor mediates positive activation in a topologically novel transcription complex. *Cell* **1989**, *56* (1), 119−129.
(238) Ansari, A. Z.; Chael, M. L.; O'Halloran, T. V. Allosteric underwinding of DNA is a critical step in positive control of transcription by Hg-MerR. *Nature* **1992**, *355* (6355), 87−89.

https://doi.org/10.1021/acs.biochem.4c00726
Biochemistry 2025, 64, 329−345